



ELSEVIER

Marine and Petroleum Geology 20 (2003) 1119–1139

Marine and
Petroleum Geology

www.elsevier.com/locate/marpetgeo

Correlation, alteration, and origin of hydrocarbons in the GCA, Bahar, and Gum Adasi fields, western South Caspian Basin: geochemical and multivariate statistical assessments

Kadir Gürgey*

Turkish Petroleum Corporation Research Center, Mustafah Kemal Mah. 2. Cad. 86, Ankara 06520, Turkey

Received 26 February 2003; received in revised form 14 October 2003; accepted 18 October 2003

Abstract

Geochemical as well as multivariate statistical analyses (PCA) were carried out on 20 crude oil samples from 'Middle' Pliocene Production Series (MPPS) of Guneshli-Chirag-Azeri (GCA), Bahar, and Gum Adasi fields in the western South Caspian Basin (SCB). PCA analysis employed to source-specific biomarkers distinguishes the oils into two types one being divided into two sub-types; Type 1 (GCA oils), Type 2A (Bahar field oils) and Type 2B (Gum Adasi field oils). Indirect oil-to-source rock correlations to available source rock data from previous studies suggest that Type 1 oils, located in the Apsheron-Balkhans uplift area, are derived from basinal shales of the Oligocene-Lower Miocene Middle Maikop Formation. Type 2A and 2B oils, located in the Gum-deniz-Bahar-Shakh-deniz trend area, are more likely derived from shelf-edge shales of the Upper Maikop Formation and the Middle-Upper Miocene Diatom Suite, respectively.

Biomarker maturity study reveals that Type 1 oils (mean %Rc = 0.78) are more mature than Type 2 oils (mean %Rc = 0.71). Source rocks, which generated these oils, were at generation depth interval between 5200 m (112 °C) and 7500 m (153 °C) at the time of expulsion. This indicates that the western SCB oils experienced significant long-range vertical migration along the deep-seated faults to accumulate in the MPPS reservoirs. Post-accumulation biodegradation process was only observed in the Guneshli field where bacterial alteration (level 4) began between 4.2 and 2.6 mybp and stopped with the deposition of the overlying impermeable Upper Pliocene Akchagyl Formation. Subsequent light hydrocarbon (C₁–C₁₆) charge into the Guneshli fields caused precipitation of asphaltenes, which is evidenced by high resin to asphaltene ratios for the present-day Guneshli oils. Evaporative-fractionation examined using the scheme of Thompson (1987) showed high correlations of the 'aromaticity' B parameter (= toluene/n-C₇) and 'parafinicity' F parameter (= n-C₇/MCH with the %Rc (maturity) and C₂₇/C₂₉ sterane ratio (organic matter type). This implies that Thompson's approach should be used with caution in the SCB. Among the several mechanisms, rapid and thick deposition of Pliocene sediments and subsequent high heating rate on the Maikop Formation and Diatom Suite is probably the most plausible way of explaining the origin of light hydrocarbons in the Guneshli and Bahar fields.

© 2004 Elsevier Ltd. All rights reserved.

Keywords: Azerbaijan; Alteration; Biomarker; Correlation; Oil; Maturation; South Caspian Basin

1. Introduction

The South Caspian Basin (SCB) covers the southern part of the Caspian Sea (Fig. 1) where petroleum exploration and production has been continuing since early 1900s. Production has been established from Upper Cretaceous to Quaternary but mainly from the sandy 'Middle' Pliocene reservoirs known as 'Productive Series' (MPPS) (Fig. 2). Currently proved reserves of the SCB is estimated at 18–35 billion barrels of oil with the basin's possible oil reserves as

high as 235 billion barrels of oil, if proven (Djevanshir & Mansoori, 2000). This number increased significantly with the recent discovery of Shakh Deniz, 70 km southwest of the Guneshli-Chirag-Azeri (GCA) oil fields. These quantitative reserve estimations given above were made on the basis of availability of trap volumes not on the expelled hydrocarbon volumes calculation of which require a considerable knowledge on source attributes such as total organic carbon (TOC), organic matter type, thermal maturity, thickness, etc.

Despite such significant future production and exploration, the geochemical data obtained on oils and possible source rocks have been incomplete or inconclusive. One

* Fax: +90-312-286-7808.

E-mail address: gurgey@petrol.tpao.gov.tr (K. Gürgey).

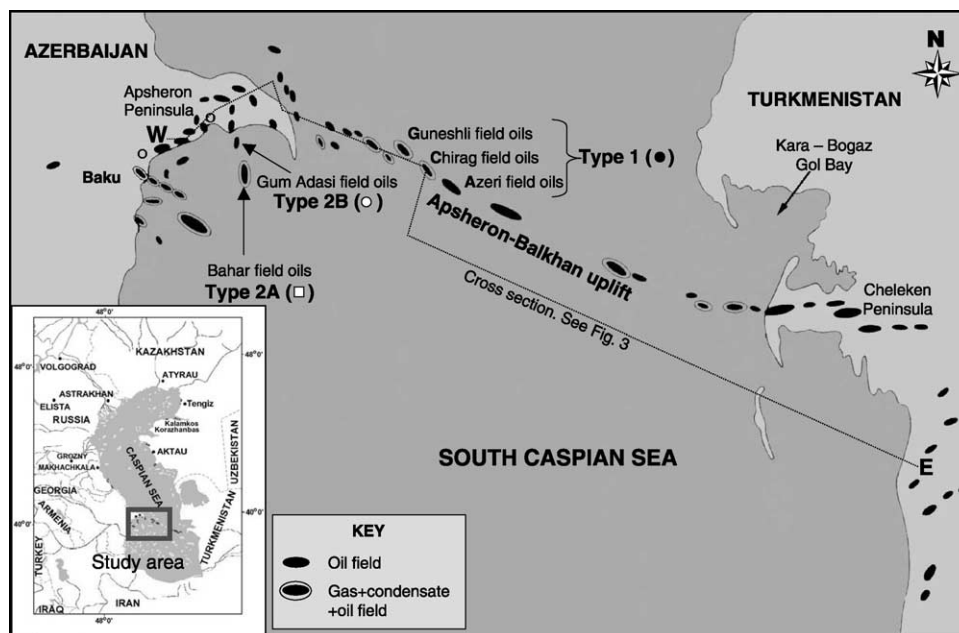


Fig. 1. A map showing location of the GCA, Bahar, and Gum Adasi oil fields in the South Caspian Basin.

reason for the lack of source rock data, particularly in offshore areas, is their very deep (10–12 km; Devlin, 2000) nature and their positioning beyond the major MPPS reservoir targets (Djavadova, Narimanov, & Rinaldi, 1997). Thus, any knowledge relevant to source attributes acquired from the available crude oil samples would have certainly help better reserve estimations and subsequently material-balance calculations.

Among the investigators, Abrams and Narimanov (1997) carried out one of the first comprehensive geochemical studies on 73 oils from the SCB (excluding Gum Adasi field oils) on the basis of biological markers and stable carbon isotopes. Accordingly, biomarker characteristics of these oils (e.g. Pr to Ph ratios > 1 , diasterane to regular sterane ratios < 1 , C_{27}/C_{29} sterane ratios $\gg 1$, C_{24} tetracyclic/ C_{26} tricyclic ratios $\ll 1$, Ts/Tm ratios < 1 , $C_{29}H/C_{30}H$ hopane ratios $\ll 1$, tricyclic/pentacyclic ratio $\ll 1$, C_{35}/C_{34} homohopane ratio < 1 , and low $C_{29} 20S/(20S + 20R)$ sterane isomerization values suggested one single oil family derived from Oligocene–Miocene marine clastic shales. However, although there are some overlapping values of the carbon isotopic values, two distinct oil families were recognized (Abrams & Narimanov, 1997). The first family oils produced from the MPPS reservoirs are isotopically heavier ($\delta^{13}C_{SAT} = -24.5$ to -27.8 per mil; $\delta^{13}C_{ARO} = -23.0$ to -26.3 per mil) and most likely related to the source rock of Middle-Upper Maikop and Middle-Upper Miocene Diatom Suite. The second family oils produced from Miocene and older reservoirs are isotopically lighter ($\delta^{13}C_{SAT} = -26.5$ to -28.5 per mil; $\delta^{13}C_{ARO} = -25.7$ to -28.2 per mil) and most likely

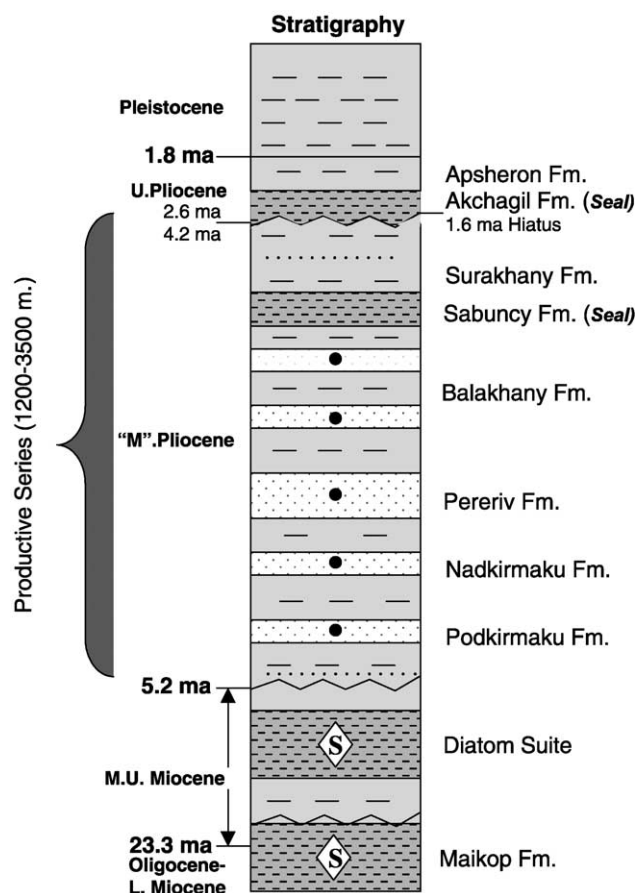


Fig. 2. Generalized stratigraphic column of the Oligocene–Pleistocene sediments showing the relationship between the major reservoir (Middle Pliocene 'Productive Series'), possible source rocks (Maikop Formation and Diatom Suite), and seal (Akchagil Formation).

correlated with the Lower Maikop Formation. Inan et al. (1998), on the other hand, studied 26 oil and 40 rock samples from eight different oil fields of the onshore Lower Kura depression, southwestern SCB. They proposed that the oils were sourced from Eocene and older units, and perhaps partially from the shales of the Maikop Formation. Abdullaev et al. (1998) reported that the Bahar field oils present similar attributes with the major oil group as described by Abrams and Narimanov (1997). However, Abdullaev et al. (1998) also pointed out that the Bahar field oils are waxier, have more C₂₉ steranes and less C₃₀ steranes than the major oil group described by Abrams and Narimanov (1997). A very small carbon isotopic range with heavy character ($\delta^{13}\text{C} = -25.0$ to -24.6 per mil) within the Bahar oils was attributed to a common source, possibly Upper Maikop Formation or Diatom Suite. More recently, Katz, Richards, Long, and Lawrence (2000) analyzed 300 outcrop samples from the onshore of Apsheron Peninsula, Azerbaijan. They argued that organic rich portion of the Maikop Formation is cyclic and contains both oil- as well as gas-prone organic rich layers. Depending on the similarity between the biomarker characteristics of extracts from this formation and those of the region's oils, they proposed that Maikop Formation is a primary source for the SCB oils. Unlike the previous studies, Katz et al. (2000) found that the Diatom Suite has only some gas potential and its contribution to region's oils is minor.

Previous investigators believe that highly variable bulk geochemical characteristics in the region's oils might have resulted from their complex and variable migration and alteration histories rather than their derivation from different source rock units. One common point among all is that after expulsion, composition of oils has been significantly altered by processes such as secondary migration, phase transformations (e.g. evaporative-fractionation), and biodegradation (Abdullaev et al., 1998; Abrams & Narimanov, 1997; Inan, Yalcin, Guliev, Kuliev, & Feizullayev, 1998; Katz et al., 2000).

This study focuses on an organic geochemical assessment of twenty crude oil samples collected from the MPPS reservoirs of the western SCB. Better understanding of thermal maturity, biodegradation, evaporative-fractionation processes, origin of light hydrocarbons, and genetic correlations among the oil samples are the main aims of this study. Genetic correlations among the oil samples are evaluated via multivariate statistical analysis. We believe that such an approach will indirectly initiate better understanding of source rock distribution and reserve estimations in the SCB.

2. Geological setting

The SCB has one of the thickest sedimentary covers known for any basin, up to 25–30 km (Devlin, 2000).

The basin is characterized by a high sedimentation rate up to 1300 m/my by during Pliocene time. The deposited sediments consist predominantly of shally-terrigeneous rocks.

The SCB is located on the Greater Caucasus-Kopet Dag portion of the Alpine-Himalayan fold belt. It is divided into three parts: (i) the Kurian sub-basin in the west; (ii) the West-Turkmenistan sub-basin in the east (e.g. limited by Kopet-Dag, the Balkhans and the coast line of the Caspian Sea along Turkmenistan and Iran); and (iii) the central part between the Kurian and West Turkmenistan sub-basins, with the Apsheron-Balkhan uplift as the northern border and the Elburs Mountains in Iran as the south border (Bagirov, Nadirov, & Lerche, 1998; Tagiyev, Nadirov, Bagirov, & Lerche, 1997). The oil fields (GCA, Gum Adasi, and Bahar fields) from which oil samples were collected are located in the western portion of the central SCB (Fig. 1).

The SCB is situated on thinned continental crust and Lower Jurassic oceanic crust formed by back-arc spreading after Triassic incorporation of Iranian and Turan blocks. From the mid-Jurassic into the Neogene, the SCB was a depression on the shelf of southern Eurasia where episodic marine restriction led to the deposition of organic-rich calcareous and diatomaceous marine black shales (Oligocene–Lower Miocene Maikop Formation and Middle-Upper Miocene Diatom Suite). The collision of Arabia and Tuarides and Pontide-Iranian blocks began to close the Caucasus Ocean in the Miocene. By the Late Miocene–Pliocene, this collision was accomplished by regional uplift of the collided terranes and subsidence of the South Caspian oceanic crust loading up to 10 km of deltaic and lacustrine clastics in the basin. This event led to the development of the MPPS reservoir facies (Fig. 2), increased burial for maturation of source rocks, liquification of basinal shales forming numerous shale diapirs, and re-structuring of anticline traps as well as the creation of new structures (Fig. 3; Guliev & Feizullayev, 1996). The main pulses of faulting/diapirism occurred in three episodes: the Early Pliocene 'Kalinskian', the Late Pliocene 'Akchaglian' and the Early Pleistocene 'Apsheronian'. Tectonic as well as mud volcano activities have been continuing through to present-day (Smale, Shikhaliyev, & Beylin, 1997).

In the central part of the SCB, extremely low values of geothermal gradient are observed (10–18 °C/1000 m) (Bagirov et al., 1998; Inan et al., 1998) compared to more usual thermal gradients of 25–35 °C/1000 m in other basins of the world. Combination of the characteristics mentioned above created abnormally high fluid pressure which caused widespread development of mud diapirism and mud volcanism (Abrams & Narimanov, 1997; Bagirov et al., 1998; Bredehoeft, Djevanshir, & Belitz, 1988; Inan et al., 1998; Tagiyev et al., 1997).

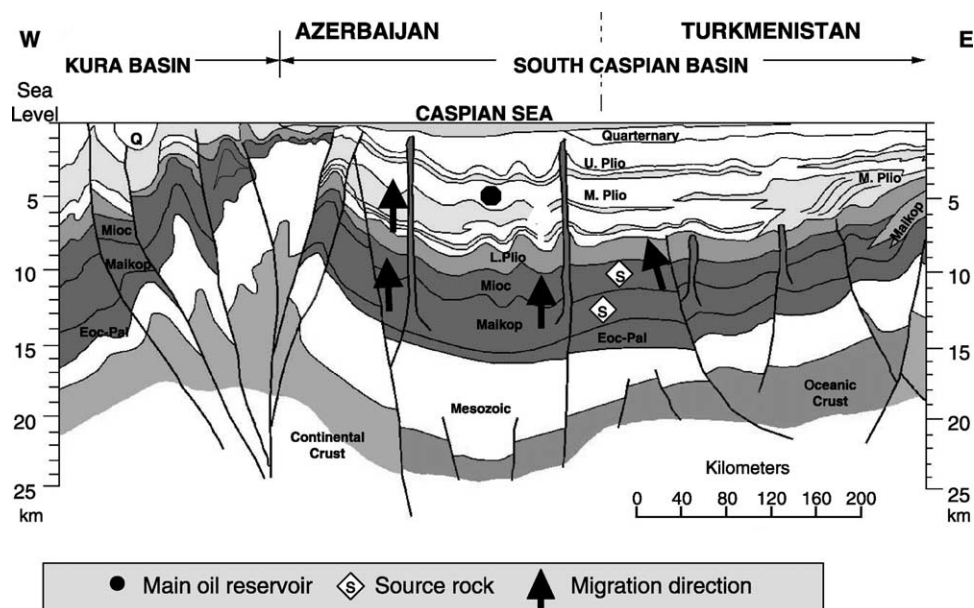


Fig. 3. A cross-section showing the source, reservoir, and mud diapirs relations across the E–W South Caspian (modified after Abrams & Narimanov, 1997).

3. Sampling, experimental, and methodology

3.1. Sampling

A total of 20 oil samples were collected from the offshore Azerbaijan sector of the western SCB; four from the Guneshli, three from the Chirag, and one from the Azeri, seven from the Gum Adasi, and five from the Bahar oil fields. Locations of the oil fields and productive stratigraphic intervals (Balakhany, Pereriv and Kirmaku formations) and abbreviation of the oil samples are shown in Figs. 1 and 2. Traps are usually in the form anticline folds, which are often cut-off by deep-seated faults, which provide a migration path for hydrocarbons. The Guneshli, Chirag and Azeri oil fields are called as ‘GCA oils’ because of their close geographic and structural association with the Apsheron-Balkhan uplift. Due to limited and incomplete subsurface information reservoir depths of the Gum Adasi field oils are missing. However, the structural and stratigraphic relationships between the Gum Adasi and Bahar fields suggest that production in the Gum Adasi field is from the MPMS as in the Bahar field.

3.2. Experimental

API gravity. Measured refractive index values by a Carl Zeiss Model Abbe Refractometer were converted to the API gravity on a previously prepared API gravity vs. refractive index calibration curves.

Asphaltene separation. About 500 mg of oil was added to 20 ml *n*-pentane in clean centrifuge tube whose dry weight was recorded. The tube was then centrifuged at 2000 rpm

for 5 min; the solution was decanted and the asphaltenes were weighted.

TLC (Thin layer chromatography)–FID (Flame Ionization Detector) Analyzer. Compound class composition, the relative percentages of saturated hydrocarbons, aromatic hydrocarbons, and resins in the deasphalted oil samples were determined using an Iatroscan™ New MK-5 TLC-FID analyzer. Three oil samples from the Bahar field, B-2, B-3, B-5, were too volatile to measure their compound class composition.

Gas chromatography (GC). GC analysis of the oils was carried out on a Varian 3700 FID gas chromatograph using a 25 m WCOT/OV-101 column (60 m × 0.25 mm i.d.). Good separation of compounds was accomplished by the oven temperature program which had a initial oven temperature of 30 °C hold for 2 min which raised to 270 °C at a rate of 4 °C/min. The oven was kept at 270 °C for 60 min until the end of each run.

Gas chromatography–mass spectrometry (GC–MS). Following isolation of the branched/cyclic fraction of the saturates of the GCA field oils, GC–MS analysis was performed using an HP 5980 gas chromatograph connected to an HP 5988A mass spectrometer (electron energy = 70 eV), controlled by a HP Chem-Station 300 data system whereas the Bahar and Gum Adasi field oils were analyzed by Finnigan Thermocrest GC Q GC-MSMS system. Similar ratios calculated for the same oil sample chromatograms obtained from HP and Finnigan instruments were close enough to make interpretations confidently. For the purpose of this study, only ions at *m/z* 217 (steranes) and *m/z* 191 (triterpanes) were examined at single ion monitoring mode (SIM). Various biomarker ratios generated from the gas and mass chromatograms were determined quantitatively by

measuring the appropriate peak heights. For both instruments, the injector temperature was maintained at 290 °C and the temperature programming was: from 50 °C (10 min) to 200 °C at 10 °C/min (15 min), at 5 °C/min to 250 °C (24 min), at 2 °C/min to 280 °C (24 min), and 1 °C to 290 °C (40 min).

Geochemical assessment of the oils was based on a multi-parameter approach that includes bulk analyses, such as API gravity measurements; compound class compositions (saturated HC%, aromatic HC%, resin%, asphaltene%), as well as molecular analyses such as gasoline range aromatics, *n*-alkanes, acyclic isoprenoids, steranes, and terpanes. The low molecular weight *n*-alkanes and aromatic hydrocarbons smaller than *n*-C₈ were lost from the GCA field oils due to unfavorable sampling, storage and/or laboratory conditions. This loss may also have happened in other oils to less degree but using the ratio of close molecular weight compounds overcomes this difficulty.

3.3. Methodology

Principal component analysis (PCA). Biomarker data obtained from the SCB oils were statistically examined through the use of PCA program of the WINSTAT[®] Statistical Package. PCA is now a well-established tool for the interpretation of multivariate dataset among the several multivariate statistical techniques (Davis, 1973). It is used to reduce the dimensionality of the data to a few important factors that best describe variations in the dataset. The major step in PCA is the extraction of the eigenvectors from the correlation matrix to get uncorrelated new variables called 'principal component' (PC) or 'factor'. Numerous application of PCA to oil-to-oil correlation studies has been documented (Eneogwe, 2003; Telnaes & Dahl, 1985; Zumberge, 1987). Detailed description of the PCA method is given in Davis (1973) and a short summary describing the main features of the method is included below. *Loading Plot*: a loading plot displays both the importance and relationship of each variable on the PC's. Interpretation of a single PC and the feature of a PC model are possible through the connection to the original variables. A variable's contribution to a PC is directly proportional to a squared loading. Thus, the distance of a variable to the origin along a PC is a quantitative measure of the importance of that variable in the PC. A variable near the origin carries little or no information while a large distance from the origin (e.g. high loading) means that the variable is important in the interpretation of the PC. In the loading plot, variables grouped together hold the same information. Also variables located on the same side of the origin are positively correlated, while variables located on the opposite sides are negatively correlated. The larger the separation of two negatively correlated variables, the stronger is the negative correlation. *Score Plot*: one of the nice features of PCA is that nearly every result can be represented graphically. The scores plot constructed by

the PCs reveals the relationships among the samples where similar samples group in clusters.

An initial treatment of the data set by PCA shows that the C₂₉H/C₃₀H and C₃₅/C₃₄ terpane ratios are statistically insignificant; hence both ratios were excluded from the further PCA treatment. Detailed results are discussed in Section 4.

4. Results and discussion

The bulk composition, gas chromatographic ratios as well as source- and maturity-related biomarker ratios for the analyzed oils are listed in Tables 1 and 2, respectively. Selected source related biomarker dataset examined through the use of PCA is also given in Table 2. Cross-correlations among the source- and maturity-specific parameters are shown in Table 3.

4.1. Oil-to-oil correlations

4.1.1. Bulk, *n*-alkane and acyclic isoprenoids

Oil-to-oil correlations require parameters, which are not altered by common geochemical processes such as biodegradation, maturation, secondary migration and evaporative-migration (Mackenzie, 1994; Peters & Moldowan, 1993). In this respect, parameters generated from bulk composition and *n*-alkanes concentrations have a tendency to change under the influence of these processes and therefore they should not be used for oil-to-oil correlation studies. However, understanding of variations in unaltered bulk and *n*-alkane compositions in a petroleum system concept may give significant clues about source type and migration pathways. Acyclic isoprenoids namely pristane and phytane are relatively resistance compounds to above mentioned processes and their usage in oil-to-oil correlations have been more common through the years (Didyk, Simoneit, Brasell, & Englinton, 1978; Eneogwe, 2003; Powell & Mckirdy, 1973).

Wide variations in bulk (e.g. API gravity and compound class composition) properties as well as *n*-alkane distribution exist between the each oil field. Among these, the GCA field oils show a relatively narrow range of bulk composition and in this respect, they seem to be different than the Bahar and Gum Adasi field oils. The GCA field oils display moderate API gravities (28–32°), relatively low saturated hydrocarbon (44–51%), moderate aromatic hydrocarbon (18–24%), high resin (23–33%), and very low asphaltene (1–2%) contents with similar saturated hydrocarbon to aromatic hydrocarbon ratios (1.86–2.61; Table 1). Bahar field oils are the lightest oils with the API gravity of 48–52°. API gravity of Gum Adasi field oils decreases with increasing depth or from the upper portion of the MPPS to lower portion of the MPPS: the Balakhany, Nadkirmaku, and Pereriv suits produce light (36–44°), moderate (27°), and relatively heavy oils (20°), respectively

Table 1
Bulk, acyclic isoprenoid, and light hydrocarbon data for the GCA, Bahar, and Gum Adasi field oils in the western South Caspian Basin

Well name	Sample ID	Oil type	Formation	Depth (m)	API	Sat%	Aro%	Res%	Asp%	Sat/Aro	Pr/Ph	Pr/n-C ₁₇	Ph/n-C ₁₈	Tol/n-C ₇	n-C ₇ /MCH	m + p Xyl/n-C ₈	n-C length	
1	Guneshli-2	G-1	1	Balakhany Suite	3039	29	45	21	33	1	2.41	1.35	12.12	8.01	nd	nd	nd	nd
2	Guneshli-170	G-2	1	Balakhany Suite	3188	30	47	18	34	1	2.61	1.25	10.62	7.55	nd	nd	nd	nd
3	Guneshli-179	G-3	1	Pereriv Suite	3337	31	47	21	32	1	2.24	1.22	33.33	20.48	nd	nd	nd	nd
4	Guneshli-182	G-4	1	Balakhany Suite	2891	30	45	24	31	1	1.86	1.24	31.04	15.08	nd	nd	nd	nd
5	Chirag-4a	C-1	1	Pereriv Suite	3020	28	46	21	33	1	2.19	1.26	0.61	0.56	nd	nd	nd	34
6	Chirag-4b	C-2	1	Pereriv Suite	2966	31	49	23	28	1	2.13	1.28	0.74	0.72	nd	nd	nd	33
7	Chirag-1	C-3	1	m	32	51	24	23	2	2.13	1.25	0.69	0.63	nd	nd	nd	32	
8	Azeri-4	A-1	1	Pereriv Suite	2796	32	44	20	33	1	2.2	1.33	0.71	0.69	nd	nd	nd	33
				mean	30	47	22	31	1	1.94	1.27	nd	nd	nd	nd	nd	33	
9	Bahar-77	B-1	2A	Balakhany Suite	4435	48	57	18	24	1	3.16	2.01	0.57	0.51	nd	nd	nd	28
10	Bahar-136	B-2	2A	Balakhany Suite	4011	51	nd	nd	nd	nd	2.01	0.39	0.49	0.94	0.83	1.01	19	
11	Bahar-139	B-3	2A	Balakhany Suite	3100	51	nd	nd	nd	nd	nd	nd	nd	1.07	0.70	1.07	18	
12	Bahar-142	B-4	2A	Balakhany Suite	m	49	50	30	20	1	1.67	2.99	0.89	0.61	0.9	0.74	1.12	21
13	Bahar-150	B-5	2A	Pereriv Suite	m	52	nd	nd	nd	nd	nd	nd	nd	1.04	0.73	1.11	18	
				mean	50	54	24	22	1	2.42	2.34	0.62	0.54	0.99	0.75	1.08	21	
14	Gum Adasi-9	GA-1	2B ?	Balakhany Suite	m	44	74	12	13	1	6.16	1.54	0.75	0.63	0.89	0.73	0.72	30
15	Gum Adasi-224	GA-2	2B	Balakhany Suite	m	44	80	12	7	1	6.66	1.44	0.77	0.59	0.78	0.77	0.69	30
16	Gum Adasi-322	GA-3	2B	Nadkirmaku	m	27	54	26	13	7	2.07	1.47	0.49	0.34	0.44	0.47	0.69	37
17	Gum Adasi-425	GA-4	2B	Balakhany Suite	m	45	79	14	6	1	5.64	1.47	0.87	0.63	0.88	0.65	0.77	31
18	Gum Adasi-438	GA-5	2B	Pereriv Suite	m	20	79	5	10	6	15.81	1.39	0.61	0.51	0.6	0.43	0.52	37
19	Gum Adasi-441	GA-6	2B	Balakhany Suite	m	36	86	4	8	2	21.5	1.33	0.54	0.51	0.79	0.67	0.49	36
20	Gum Adasi-1702	GA-7	2B	Kirmaku	m	27	58	13	25	4	4.46	1.43	0.58	0.49	nd	nd	nd	37
				mean	35	73	12	12	3	9	1.44	0.66	0.63	0.73	0.62	0.65	34	

Key to the parameters in order: API, API gravity; Sat%, saturated; HC%, Aro%, aromatic HC%; Res%, resin%; Asp%, asphaltene%; Pr/Ph, pristane/phytane; pristane/n-C₁₇, pristane/n-octadecane; Ph/n-C₁₈, phytane/n-dodacane; Tol/n-C₇, toluene/n-heptane; n-C₇/MCH, n-heptane/methylcyclohexane; m + p Xyl/n-C₈, meta + orta xylene/n-octane; n-C length, n-alkane carbon chain length; m, missing.

Table 2
Selected source- and maturity-specific biomarker data for the GCA, Bahar, and Gum Adasi field oils

Sample ID	Oil type	C ₂₇ :C ₂₈ :C ₂₉ ^a	C ₂₇ /C ₂₉ ^a	C ₂₈ /C ₂₉ ^a	C ₂₃ /C ₃₀ H ^a	C ₂₄ /C ₂₆ ^a	Ts/Ts + Tm ^a	OL/C ₃₀ H ^a	C ₂₉ H/C ₃₀ H ^b	C ₃₀ H/C ₂₉ Ts ^a	HHI ^a	C ₃₅ /C ₃₄ ^b	% 22S ^c	C ₃₀ M/ C ₃₀ H ^c	% 20S ^c	% BB ^c	%Rc ^c	
1	G-1	1	39:33:28	1.39	1.18	0.4	1.00	0.47	3	0.55	0.33	5	0.67	0.62	0.13	0.49	0.49	0.80
2	G-2	1	36:32:32	1.13	1.00	0.57	0.78	0.45	2	0.62	0.42	5	0.73	0.55	0.11	0.52	0.52	0.85
3	G-3	1	38:33:29	1.31	1.14	0.17	1.00	0.46	3	0.54	0.33	4	0.58	0.58	0.14	0.46	0.47	0.75
4	G-4	1	38:34:28	1.36	1.21	0.38	0.86	0.48	3	0.54	0.31	6	0.67	0.58	0.14	0.46	0.48	0.75
5	C-1	1	38:34:29	1.31	1.17	0.24	0.80	0.49	3	0.53	0.33	4	0.69	0.61	0.14	0.45	0.49	0.73
6	C-2	1	34:36:30	1.13	1.20	0.21	0.80	0.45	3	0.56	0.33	4	0.55	0.61	0.13	0.51	0.48	0.85
7	C-3	1	35:35:30	1.17	1.17	0.57	0.86	0.46	4	0.52	0.39	5	0.67	0.58	0.13	0.47	0.48	0.76
8	A-1	1	35:35:30	1.17	1.17	0.24	1.25	0.45	4	0.64	0.38	3	0.59	0.58	0.15	0.46	0.47	0.75
		Mean	37:34:30	1.25	1.16	0.35	0.92	0.46	3	0.55	0.35	5	0.64	0.59	0.13	0.48	0.49	0.78
9	B-1	2A	33:30:37	0.89	0.81	0.11	0.75	0.57	5	0.45	0.38	3	0.51	0.60	0.12	0.51	0.54	0.77
10	B-2	2A	29:30:41	0.71	0.73	0.2	0.58	0.45	12	0.48	0.48	10	0.81	0.53	0.13	0.41	0.47	0.67
11	B-3	2A	29:29:42	0.69	0.69	0.01	1.98	0.51	17	0.61	0.46	9	0.81	0.55	0.17	0.44	0.45	0.72
12	B-4	2A	31:33:36	0.86	0.92	0.15	0.88	0.52	20	0.56	0.07	6	0.58	0.59	0.15	0.47	0.37	0.77
13	B-5	2A	26:28:46	0.57	0.61	0.11	0.75	0.55	13	0.65	0.41	13	0.83	0.57	0.17	0.38	0.33	0.64
		Mean	30:30:40	0.74	0.75	0.12	0.99	0.52	13	0.55	0.36	8	0.71	0.57	0.15	0.44	0.43	0.71
14	GA-1	2B	29:35:36	0.81	0.97	0.6	0.75	0.56	7	0.56	0.39	3	0.42	0.57	0.13	0.49	0.48	0.81
15	GA-2	2B	14:38:48	0.37	0.79	0.51	0.62	0.48	4	0.6	0.43	1	0.11	0.60	0.14	0.44	0.41	0.72
16	GA-3	2B	20:30:50	0.40	0.60	0.1	0.83	0.49	6	0.59	0.42	7	0.73	0.51	0.19	0.37	0.3	0.62
17	GA-4	2B	12:39:48	0.25	0.81	0.26	0.85	0.56	7	0.66	0.44	7	0.61	0.60	0.11	0.48	0.41	0.79
18	GA-5	2B	19:40:41	0.46	0.92	0.1	0.53	0.52	3	0.49	0.56	7	0.73	0.58	0.13	0.41	0.43	0.66
19	GA-6	2B	21:32:47	0.45	0.68	0.01	0.63	0.61	14	0.59	0.64	6	0.63	0.58	0.25	0.45	0.44	0.72
20	GA-7	2B	22:35:43	0.51	0.81	0.12	1.01	0.48	10	0.61	0.31	10	0.83	0.52	0.19	0.32	0.31	0.56
		Mean	20:35:45	0.46	0.80	0.24	0.75	0.53	7	0.59	0.46	6	0.58	0.57	0.16	0.42	0.40	0.70

Key to the parameters in order: C₂₇:C₂₈:C₂₉, C₂₇:C₂₈:C₂₉ 5 α , 14 α , 17 α , 20R-cholestanes (*m/z* 217); C₂₇/C₂₉, 5 α , 14 α , 17 α , 20R-cholestane/5 α , 14 α , 17 α , 20R-24-ethyl-cholestane (*m/z* 217); C₂₈/C₂₉, 5 α , 14 α , 17 α , 20R-cholestane/5 α , 14 α , 17 α , 20R-ethyl-cholestane (*m/z* 217); C₂₃/C₃₀H, C₂₃ tricyclic terpane/17 α ,21 β -hopane (*m/z* 191); C₂₄/C₂₆, C₂₄ tetracyclic terpane/C₂₆ tricyclic terpane (*m/z* 191); Ts/Ts + Tm, 17 α (H)-22,29,30-trisnorhopane/17 α (H)-22,29,30-trisnorhopane + 18 α (H)-22,29,30-trisnorhopane (*m/z* 191); OL/C₃₀H, 18 α (H)-oleanane/C₃₀ 17 α ,21 β -hopane) \times 100(*m/z* 191); C₂₉H/C₃₀H, 17 α ,21 β -30-norhopane/17 α ,21 β (H)-hopane (*m/z* 191); C₃₀H/C₂₉Ts, 17 α (H)-diahopane/18 α (H) 30-norneohopane (*m/z* 191); HHI, homohopane index, (C₃₅/C₃₅ + C₃₄ + C₃₃ + C₃₂ + C₃₁) \times 100(*m/z* 191); C₃₅/C₃₄, C₃₅ 17 α ,21 β -pentakishomohopane/C₃₄ 17 α ,21 β -30-tetrakishomohopane (*m/z* 191); % 22S, 22S/22S + 22R, C₃₂ 27 α , 21 β (H), 22S-dishomohopane/17 α ,21 β -22S-dishomohopane + 17 α ,21 β -22R-dishomohopane (*m/z* 191); C₃₀M/C₃₀H, C₃₀ 17 β 21 α moretane/C₃₀ 17 α ,21 β (H)-hopane (*m/z* 191); % 20S, 20S/20S + 20R, C₂₉ 5 α , 14 α , 17 α , 20S-24-ethyl-cholestane/C₂₉ 5 α , 14 α , 17 α ,20R-24-ethyl-cholestane + C₂₉ 5 α , 14 α , 17 α , 20S-24-ethyl-cholestane (*m/z* 217); % $\beta\beta$, $\beta\beta$ / $\beta\beta$ + $\alpha\alpha$, 5 α , 14 β , 17 β , 20S-24-ethyl-cholestane + 5 α , 14 β , 17 β , 20S-24-ethyl-cholestane/5 α , 14 β , 17 β , 20S-24-ethyl-cholestane + 5 α , 14 β , 17 β , 20R-24-ethyl-cholestane + 5 α , 14 α , 17 α , 20R-24-ethyl-cholestane + 5 α , 14 α , 17 α , 20S-24-ethyl-cholestane (*m/z* 217); %Rc = % Ro = 0.49 (20S/20R) + 0.33 (Zumberge, J.E. 1984, personal communication).

^a Source-specific parameters used in the PCA.

^b Parameters not used in the PCA.

^c Maturity-specific parameters not used in the PCA.

(Table 1; Fig. 2). These variations in API gravity go parallel to maturity changes rather than changes created by phase transformations (Section 4.2.4). In fact, a role of geochromatographic-migration could also be thought to explain API gravity variations in the Gum Adasi oils and/or in the SCB oil fields. However, due to poor depth control of the reservoired oils, geochromatographic-migration has not been considered further.

Bulk, *n*-alkane, and acyclic isoprenoids could be subjected to possible pre- and post-accumulation alterations that may be ended with significant changing in primary oil compositions. It is noteworthy to mention that, a Sat-Aro-(Resins + Asph) ternary diagram given in Fig. 4 shows three oil groupings which correspond to the each individual oil fields: GCA, Bahar, and Gum Adasi. This may be explained with an occurrence of unique pre- and post-accumulation alteration processes on each individual oil grouping, in other words, geochemical source rock attributes play only a minor effect on the present day bulk composition analyzed oils.

Relative distributions of *n*-alkanes for each oil field are distinctive with respect to their peak carbon number, *n*-alkane carbon chain length and their percentage distributions (Table 2; Fig. 5). Even though, the Gum Adasi oils show considerable differences in their compound class composition they show consistently similar *n*-alkane distributions (Fig. 5c). Interestingly enough, within the closely associated GCA oils, the Guneshli oils differ from the Chirag and Azeri oils on the basis of their carbon

number maximum at *n*-C₁₂ and *n*-C₁₃ and a narrow carbon number chain length from *n*-C₇ to *n*-C₂₁ (Fig. 5). Differences of the Guneshli oils having higher ratios of Pr/*n*-C₁₇ (12.12–33.33) and Ph/*n*-C₁₈ (8.01–20.48) from the rest of other oils (Pr/*n*-C₁₇ = 0.39–0.89 and Ph/*n*-C₁₈ = 0.34–0.72) clearly indicate that the Guneshli field oils have been biodegraded (Fig. 6). However, despite this apparent biodegradation evidence, the Guneshli field oils still contain appreciable amount of low molecular weight hydrocarbons reflecting probably a second charge of hydrocarbon input (Section 4.2.3).

The Pr/*n*-C₁₇ vs. Ph/*n*-C₁₈ diagram given in Fig. 6, beside biodegradation, could also provide information about the source material type, environment of deposition, and maturity (Connan & Cassau, 1980; Peters, Frase, Amris, Rustanto, & Hermento, 1999). This diagram infers that all the oils contain probably a mixed terrigenous higher plant and marine algal organic matter deposited under oxic to sub-oxic conditions. Interestingly, the biodegraded Guneshli field oils, which plot at the upper right hand side of the diagram, look as a separate group but appear to have similar source suggesting a possible genetic relation with the unbiodegraded oils. Terrigenous input and oxic conditions of depositional environment for the source rock of the Bahar field oils are further supported by their relatively high Pr/Ph ratios (2.01–2.99) whereas moderate the Pr/Ph ratios for the GCA (1.22–1.35), and Gum Adasi (1.33–1.57) field oils (Table 1) may show oxic to sub-oxic conditions in their source rock depositional conditions.

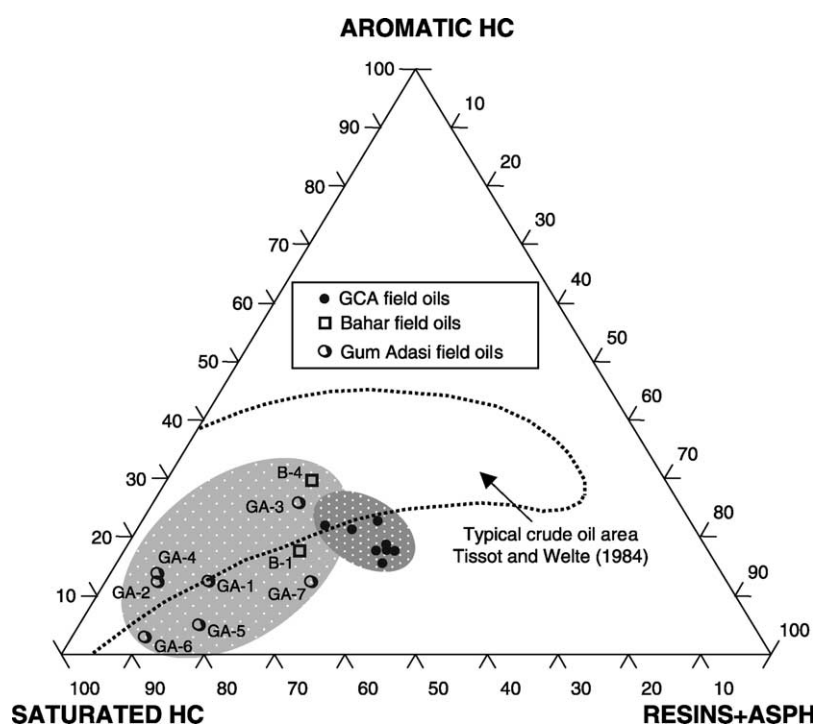


Fig. 4. Ternary diagram showing the class compound distributions in the GCA, Bahar, and Gum Adasi field oils. Typical crude oils fall within solid-line area (Tissot & Welte, 1984). Sample and variable codes as in Tables 1 and 2.

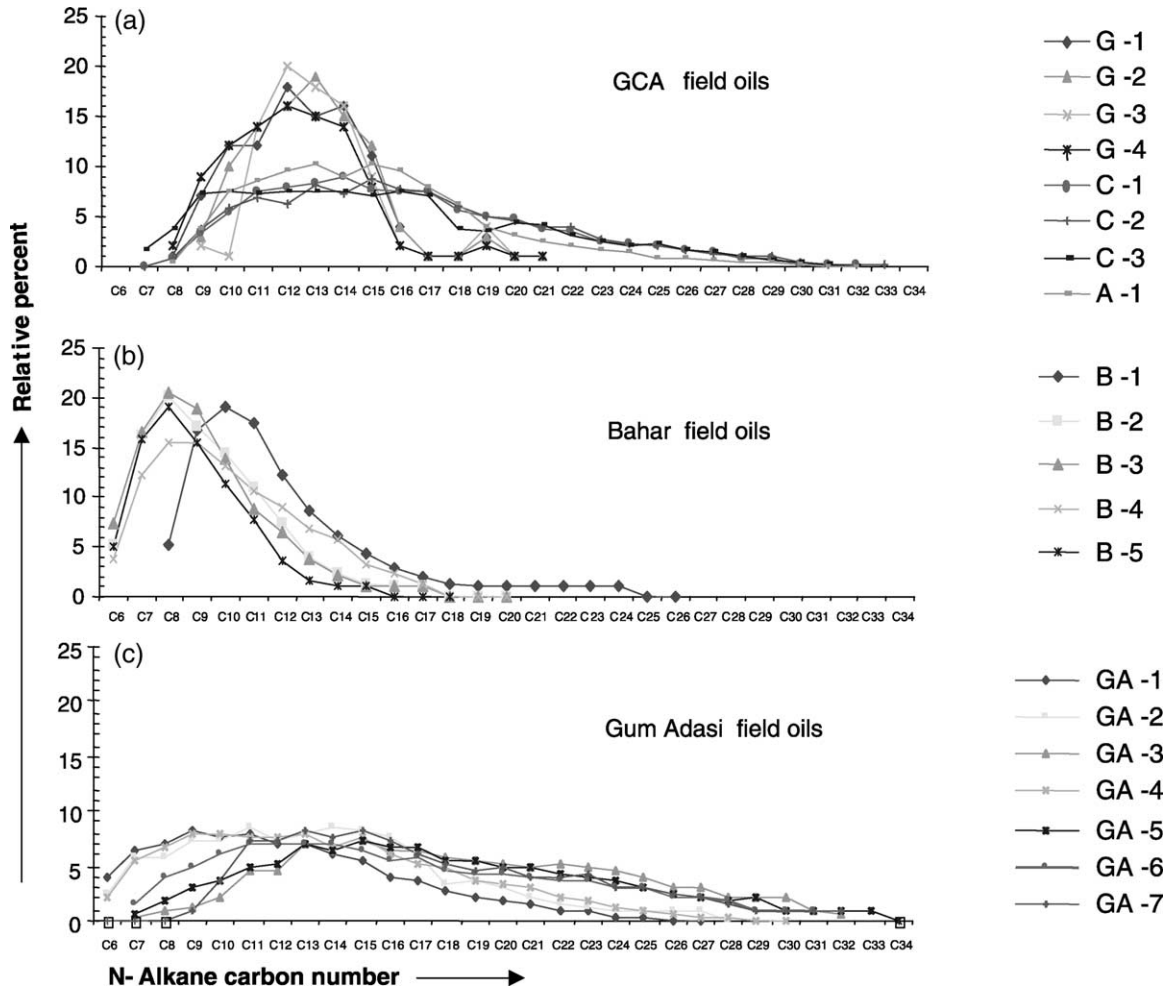


Fig. 5. Comparison of n -C₆– n -C₃₄ alkane percent distributions in the (a) GCA, (b) Bahar, and (c) Gum Adasi field oils. Sample codes as in Tables 1 and 2.

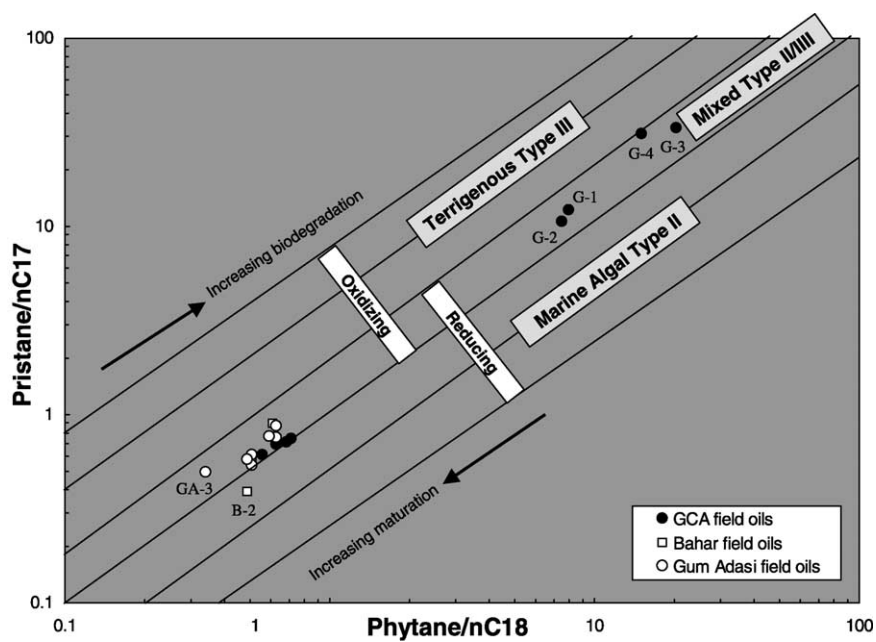


Fig. 6. Plot of Pr/ n -C₁₇ vs. Ph/ n -C₁₈ ratios from whole-oil gas chromatograms showing organic matter type, biodegradation, maturation, and conditions existed in the source of the GCA, Bahar, and Gum adasi oils (Connan & Cassau, 1980; Peters et al., 1999). Sample and variable codes as in Tables 1 and 2.

Table 3
Correlation matrix of the source- and maturity-specific parameters and the first two principal components PC1 and PC2

	% C ₂₇	% C ₂₈	% C ₂₉	C ₂₇ /C ₂₉	C ₂₈ /C ₂₉	C ₂₃ /C ₃₀ H	C ₂₄ /C ₂₆	Ts/Ts + Tm	OL/C ₃₀ H	C ₂₉ H/C ₃₀ H	C ₃₀ *H/C ₂₉ Ts	HHI	C ₃₅ /C ₃₄	20S/20 + 20R	PC1	PC2
% C ₂₇	-0.33															
% C ₂₈	-0.91	-0.07														
% C ₂₉	0.97	-0.18														
C ₂₇ /C ₂₉	0.69	0.44	-0.95													
C ₂₈ /C ₂₉	0.23	0.38	-0.40	0.78												
C ₂₃ /C ₃₀ H	0.24	-0.29	-0.14	-0.33	0.57	1										
C ₂₄ /C ₂₆	-0.46	-0.09	0.52	-0.47	-0.03	-0.29	1									
Ts/Ts + Tm	-0.26	-0.45	0.47	-0.35	-0.50	-0.33	-0.17	1								
OL/C ₃₀ H	-0.46	-0.02	0.49	-0.45	-0.43	0.03	0.24	0.43	1							
C ₂₉ H/C ₃₀ H	-0.45	-0.01	0.47	-0.49	-0.39	-0.16	-0.16	0.32	-0.09	1						
C ₃₀ *H/C ₂₉ Ts	-0.24	-0.43	0.42	-0.32	0.55	-0.50	0.14	0.13	0.56	0.35	1					
HHI	0.18	-0.44	-0.01	0.12	-0.18	-0.44	0.26	-0.09	0.27	0.09	0.80	1				
C ₃₅ /C ₃₄	0.46	0.14	-0.56	0.44	0.57	0.42	-0.01	0.01	-0.31	-0.19	-0.66	-0.43	1			
20S/20S + 20R	0.96	-0.19	-0.94	0.96	0.75	0.29	0.34	-0.59	-0.28	-0.38	-0.27	0.13	0.42	1		
PC1	-0.05	0.79	-0.28	0.08	0.57	0.71	-0.54	-0.22	-0.79	-0.21	-0.70	-0.60	0.38	0.01	1	
PC2																1

Absolute linear correlations >0.50 are highlighted. Descriptions of the parameters are given in Table 2.

4.1.2. Biomarkers

Biomarkers, namely steranes and terpanes, are less affected by the geochemical alteration processes. Furthermore, they are sensitive to source rock attributes such as depositional conditions (e.g. salinity, oxicity, anoxicity, etc.) lithology, maturity, organic matter type and quality, and maturation (Mackenzie, 1984; Seifert & Moldowan, 1978, 1979). Such features have made biomarkers potentially applicable to oil-to-oil correlations (Johnson, Greene, Zinniker, Moldowan, & Hendrix, 2003; Peters & Moldowan, 1993).

Initially, the biomarker data listed in Table 2 were visually evaluated, and found that the GCA, Bahar, and Gum Adasi field oils show variety of similarities: *m/z* 191 chromatograms show 17 α , 21 β -hopane distributions dominated by C₃₀ hopane. Low ratios of C₂₉H to C₃₀H (0.45–0.66) are an indicator of clastic shaly nature of the source (Palacas, Anders, & King, 1984). A sharp decrease in intensity from C₃₁ to C₃₅ homohopanes, and low ratios of C₃₅ to C₃₄ homohopanes (0.11–0.83) indicate the prevailing oxic to sub-oxic (high Eh) conditions during deposition (Peters & Moldowan, 1993) as well as low quality organic matter (e.g. organic matter with low hydrogen index; Dahl, Moldowan, Teerman, McCaffrey, & Sundararaman, 1994). The presence of higher plant (e.g. angiosperm) biomarker 18 α -(H) oleanane in all the oils suggests source rocks with Late Cretaceous to Tertiary in age and higher plant input (Grantham, Posthuma, & Baak, 1983). Presences of C₃₀ regular steranes, which are abundant in algal-rich marine-sourced oils, confirm that the source rock of the SCB oils was deposited in marine environment (Abrams & Narimanov, 1997). These similar characteristics clearly show that analyzed SCB oils were most likely generated from source rocks with similar facies characteristics (e.g. Marine Tertiary clastic source rocks containing varying amount of terrestrial source material deposited in oxic to sub-oxic conditions).

It appears that the close similarity among the biomarker data (Table 2) and *m/z* 191 terpane and 217 sterane chromatograms of the oils do not allow us to distinguish the SCB oils on simple binary and/or ternary diagrams. In order to overcome this difficulty and to provide better understanding of the quantitative relations among 14 variables (Steranes: % C₂₇, % C₂₈, % C₂₉, C₂₇/C₂₉, and C₂₈/C₂₉. Hopanes: C₂₃/C₃₀H, C₂₄/C₂₆ and, Ts/Ts + Tm, OL/C₃₀H, C₂₉H/C₃₀H, C₃₀*H/C₂₉Ts, HHI, C₃₅/C₃₄, 20S/20S + 20R; Table 2), the correlation matrix has been constructed (Table 3). Principle components, PC1 and PC2 (Section 4.1.3) were also added to Table 3.

There are several very negative and positive correlation coefficients among the variables in Table 3. This is especially true for the negative correlations between % C₂₇ vs. % C₂₉; C₂₇/C₂₉ vs. % C₂₉; C₂₈/C₂₉ vs. % C₂₉ steranes, which may be attributed to presence of negative correlation between terrigenous (C₂₉) and marine (C₂₇; C₂₈) organic matter in general (Huang & Meinschein, 1979).

Very low negative correlation (-0.26) between % C_{27} sterane and $OL/C_{30}H$ is difficult to explain since C_{27} steranes are thought to be associated marine algae and OL (oleanane) typically reflects a terrigenous origin (Grantham et al., 1983). Therefore, one would expect higher negative correlation between the two variables. Similarly, significant positive correlation ($+0.56$) between homohopane index (HHI) and $OL/C_{30}H$ is also unexpected. HHI for oils has shown to be positively correlated with the hydrogen index of the associated kerogen and therefore HHI decreases with decreasing terrigenous organic matter content (Dahl et al., 1994). This may be partially explained by considering decreasing HHI values with increasing thermal maturity (Dahl et al., 1994; Peters & Moldowan, 1993). In fact, high negative correlation (-0.66) between HHI and maturity parameter $20S/(20S + 20R)$ (Table 3) verifies this hypothesis.

4.1.3. PCA analysis

PCA applied to dataset (Table 2) resulted with two significant PC's (PC1 and PC2) accounting for 67.24% of the total variance in the data. Loading and score plots constructed on the basis of the first (PC1, 45.30%) vs. the second (PC2, 21.94%) PC's display the contribution of each variable related to PC1 and PC2 (Fig. 7a) and the genetic relations among the oil samples again in the plane of the PC1 and PC2 (Fig. 7b).

As shown in the score plot in Fig. 7b, two distinct oil types along the PC1 are recognized: Type 1 (8 oils from GCA fields) and Type 2 (12 oils from Bahar and Gum Adasi fields). When the distribution of source-specific parameters in Fig. 7a is interpreted, PC1 appears to be mostly related to the source organic facies. At the right-hand side of the PC1 axis, PC1 is characterized by marine algal organic matter and diatoms designated by % C_{27} , C_{27}/C_{29} , and C_{28}/C_{29} (e.g. correlation coefficients with PC1 are $+0.96$, $+0.96$, and $+0.75$, respectively; Table 3; Fig. 7a) that are enriched in the Type 1 oils while at the left hand side of the PC1 axis, PC1 is characterized by terrestrial organic matter inferred by % C_{29} , $C_{30}^*H/C_{29}Ts$, and $Ts/Ts + Tm$ (e.g. correlation coefficients with PC1 are -0.94 , -0.60 , and -0.59 , respectively, Table 3) that are enriched in the Type 2A and 2B oils (Fig. 7a). It has to be emphasized that strong loading of C_{28}/C_{29} ratios on the Type 1 oils may be related to phytoplankton assemblages including diatoms, coccolithophores and dinoflagellates (Grantham & Wakefield, 1988). On the other hand, the $C_{30}^*H/C_{29}Ts$ ratio depends strongly on environment of deposition, and that oils derived from shales deposited under oxic–suboxic conditions will show higher ratios than those derived from source rocks deposited under anoxic conditions (Philp & Gilbert, 1986; Volkman, Alexander, Kagi, Noble, & Woodhouse, 1983). The $Ts/Ts + Tm$ ratio is both maturity- and source-dependent. Since the ratio begins to increase at about peak oil generation ($>0.9\%$ Ro: Van Grass, 1990) and the analyzed oils show $R_o < 0.90$ (Section 4.2.1), $Ts/ts + Tm$ ratio is

assumed to be largely source dependent in the SCB. Additionally, $Ts/Ts + Tm$ ratio appears to be sensitive also to clay-catalyzed reactions (Rullkotter, Spiro, & Nissenbaum, 1985) and supports clay-rich mineralogy of the source rock of the Type 2A and 2B oils. Thus, strong negative loading of $C_{30}^*H/C_{29}Ts$ ratios on the Type 2A and 2B oils (Table 2) suggests that the source of these oils was deposited under stronger oxic–suboxic conditions compare to the Type 1 oils (Fig. 7b).

Along the PC2, the Type 2 oils are clearly divided into two sub-types: Type 2A (five oils from Bahar fields) and Type 2B (seven oils from the Gum Adasi field). PC2 displays negatively correlated two groups of variables: % C_{28} and $C_{23}/C_{30}H$ ratio (e.g. correlation coefficients with PC2 are $+0.79$ and $+0.71$, respectively; Table 3; Fig. 7a), and HHI, and $OL/C_{30}H$, and C_{24}/C_{26} ratios (e.g. correlation coefficients with PC2 are -0.70 and -0.79 , and -0.54 , respectively; Table 3). It can therefore be expected that PC2 is also sensitive to organic facies comprising by diatom (higher % C_{28} Grantham & Wakefield, 1988) and angiosperms at the bottom of the axis (higher $OL/C_{30}H$: Grantham, 1983). In this respect, we propose that the optimal parameters to separate the Type 2A from 2B oils along the PC2 axis are the C_{28} percentage and $OL/C_{30}H$ ratios.

Locations of the oils in two different geologic provinces further support the presence of two distinct oil types in the SCB. The GCA fields of Type 1 oils, which are sourced predominantly from better preserved marine algal and diatom-rich organic matter, are located in the Apsheeron Balkhans uplift trend area whereas the Bahar (Type 2A) and Gum Adasi (Type 2B) fields of Type 2 oils, which are sourced predominantly from mixed continental higher plants and marine phytoplankton (diatom)-rich organic matter are located in the Gum-deniz-Bahar-Shakh-deniz anticline trend area of the southern Apsheeron Trough (Narimanov, Akperov, & Abdullaev, 1998).

4.2. Assessments of thermal maturation, biodegradation and origin of light hydrocarbons

4.2.1. Thermal maturity of oils

As will be discussed below, oils accumulated in the MPPS reservoirs have migrated considerable distance in an up-dip direction from the underlying source rocks. That is, temperature in the MPPS oil reservoirs has never exceeded the temperature of the underlying source rocks. Therefore, thermal maturity of the oils is considered here to represent the maturity of the source rock at the time of oil expulsion. In this study, the following biomarker maturity indicators are used; $C_{29} 20S/(20S + 20R)$, $\beta\beta/(\beta\beta + \alpha\alpha)$ sterane, $C_{32} 22S/(22S + 22R)$ hopane, $C_{30}M/C_{30}H$ (moretane/hopane) ratios (Mackenzie, 1984; Peters & Moldowan, 1993).

The $C_{29} 20R$ to $20S$ conversion of $\alpha\alpha$ steranes cause $20S/(20S + 20R)$ ratio increase with increasing maturity (Mackenzie, Patience, & Maxwell, 1980), usually reaching

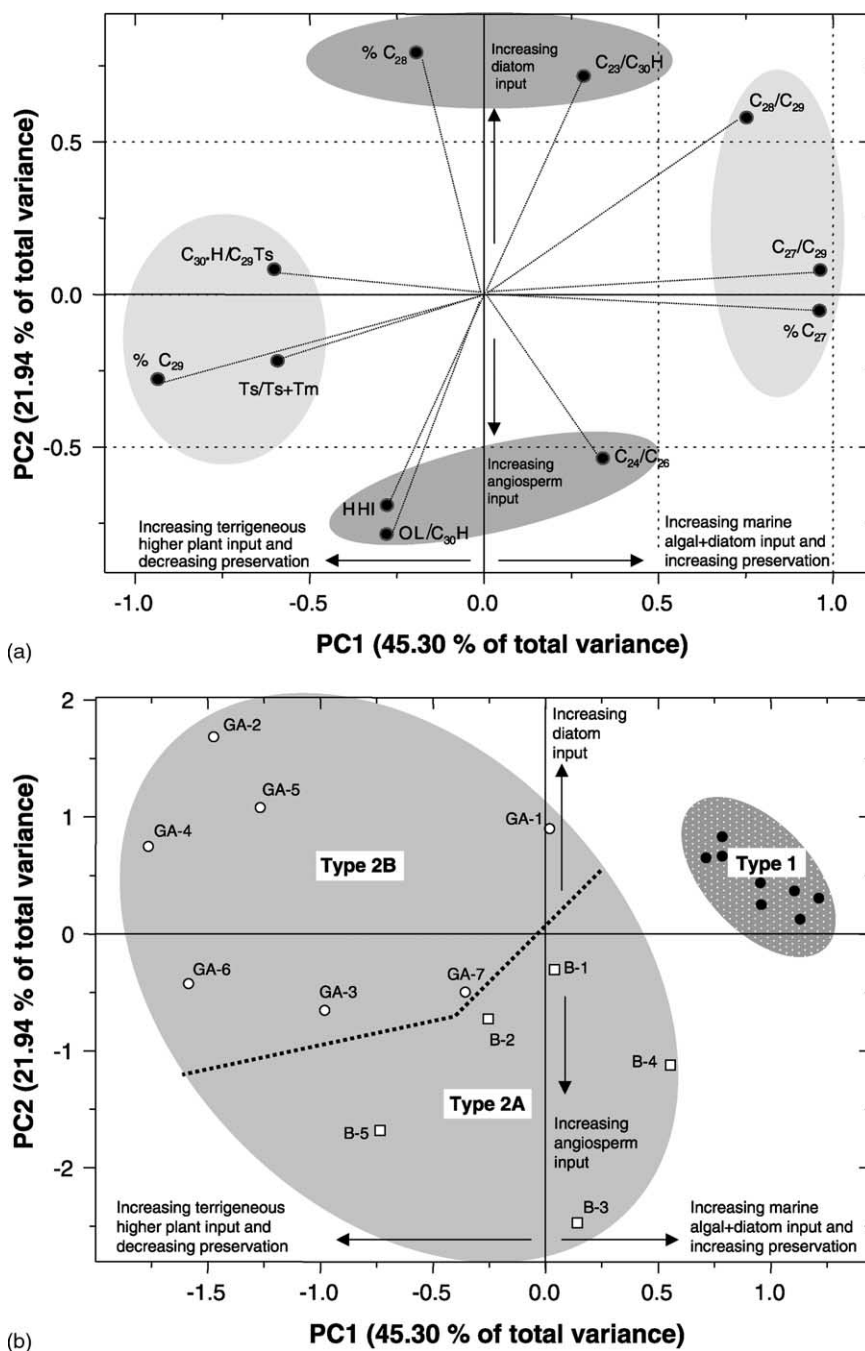


Fig. 7. Results of multivariate data analysis of the 11 source-specific biomarker parameters vs. 20 oil samples from the GCA, Bahar, and Gum Adasi fields: (a) Loadings and (b) scores on PC1 vs. PC2 from principal component analysis. Samples and variable codes as in Tables 1 and 2.

a steady state value of 0.55 near main oil generation stage. The C_{29} sterane isomerization at C14 and C17 from $\alpha\alpha$ configuration to $\beta\beta$ configuration is expressed as $\beta\beta/(\beta\beta + \alpha\alpha)$ ratio that reaches a steady state value of 0.70 around peak oil generation (Mackenzie et al., 1980; Ramon & Dzou, 1999). This ratio is somewhat slower to reach equilibrium than the $20S/(20S + 20R)$ ratio, thus making it effective at higher levels of maturity. The C_{32} homohopane maturity ratio $22S/(22S + 22R)$ reaches equilibrium of about 0.57–0.60 when the onset of hydrocarbon generation

has been reached or surpassed. The $C_{30}M/C_{30}H$ ratio, on the other hand, decreases with increasing maturity from about 0.8 in immature source rock to 0.15 in mature source rocks or oils (Mackenzie et al., 1980).

The sterane $20S/(20S + 20R)$ and $\beta\beta/(\beta\beta + \alpha\alpha)$ isomerization ratios calculated for the SCB oils range from 0.32 to 0.52 and 0.30 to 0.54, respectively, which are well below the steady state values given above. High correlation coefficient ($r = +0.81$) between $20S/(20S + 20R)$ and $\beta\beta/(\beta\beta + \alpha\alpha)$ ratios increase the reliability of the maturity

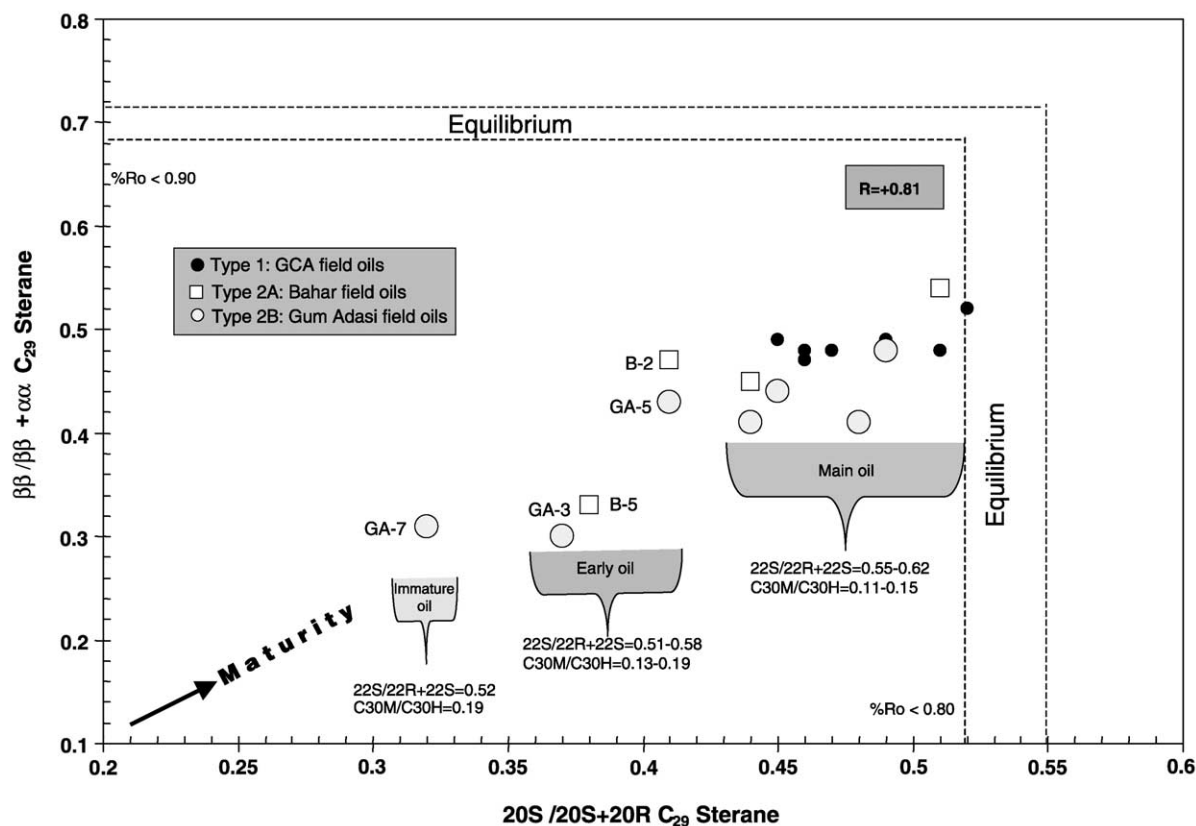


Fig. 8. Maturity evaluation of the GCA, Bahar, and Gum Adasi field oils based on sterane isomerization ratios. Note the a good correlation between the two isomerization parameters.

assessments (Fig. 8). Furthermore, Type 1 oils seem more mature than the Type 2A and 2B oils (Figs. 8). It is interesting to note that although Type 2B oils are produced from the same oil field, they display large range of maturity levels ($\% R_c = 0.56\text{--}0.81$). Large range of maturity levels could be a product of continuous expulsion from their respective source rocks at different thermal maturities. Accordingly, three separate maturity groupings of the oils shown in Fig. 8 may refer three main episodes of expulsion from corresponding source rocks: (1) pulse in immature stage (GA-7 oil), (2) pulse in early oil stage (GA-3, B-5, GA-5, and B-2 oils), and (3) pulse in main oil stage (remaining oils). Initiation of hydrocarbon generation and expulsion for the GA-7 oil appear to occur at significantly low maturity of 0.56% Rc (Section 4.2.2). It is likely that residual water (related to rapid subsidence) in the source rock would contribute to aquathermal overpressure to promote such an expulsion event at early maturity levels (Wavrek et al., 1996).

Homohopane 22S/(22S + 22R) isomerization ratios of the SCB oils range from 0.51 to 0.62. Most of the oil samples excluding G-1, C-1, G-2, B-1, GA-2, and GA-4, having the 22S/(22S + 22R) ratios of less than the equilibrium value of 0.60 appear to be early mature with respect to oil generation stages (e.g. $\% R_o < 0.60$; Waples

and Machihara, 1990). Significantly low and inverse correlation ($r = -0.38$) found between the 22S/(22S + 22R) and $C_{30}M/C_{30}H$ ratios implies that both ratios are affected by other sources in addition to thermal maturity, for example they could be contaminated from other immature hydrocarbons along the secondary migration pathways. However, all the oils with the exception of the GA-6 oil (0.25) show $C_{30}M/C_{30}H$ ratios between 0.11 and 0.19, which are characteristic values for oils derived from low mature Tertiary source rocks (Grantham, 1986).

4.2.2. Prediction of source rock maturation and depth

An attempt was made to predict vitrinite reflectance equivalent ($\% R_c$) values of the oil samples by using C_{29} 20/20R sterane ratio of the oils. This is a useful way of estimating thermal maturity of the source rocks at the time of expulsion. The $\% R_c$ values of the SCB oils are calculated using the relationship between $\% R_o$ of the kerogen and 20S/20R sterane ratio of the extract from the same sample: $\% R_c = 0.49 (20S/20R) + 0.33$ (Zumberge, J.E. 1984, personal communication). This equation was formulated based on a calibration between the measured vitrinite reflectance values ($\% R_o$) of the kerogen and 20S/20R ratios of relevant extracts from a number of rock samples with various thermal maturities and depositional

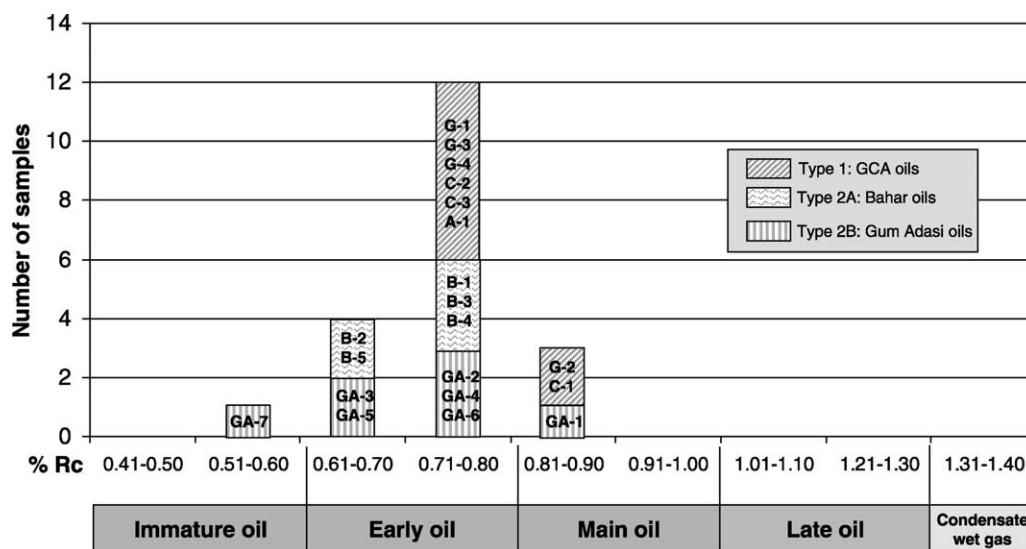


Fig. 9. Calculated vitrinite reflectance (%Rc) values and their corresponding oil generation stages for GCA, Bahar, and Gum adasi field oils. Sample codes as in Tables 1 and 2.

environments. Using the formula given above, the % Rc values of the western SCB oils range from 0.56 to 0.85 (Table 2). A histogram showing main hydrocarbon generation stages and their corresponding SCB oils is given in Fig. 9. In this respect, previously estimated % Rc values appear to be similar to those of ours excluding % Rc = 0.57 for the GA-7 oil sample. Reported %Rc values by Abrams and Narimanov, 1997, Abdullaev et al. (1998), Inan et al. (1998), Katz et al. (2000) and Wavrek et al. (1996) are as follows: 0.70–0.80, 0.75–0.85, 0.79–0.92, 0.70–0.80, and 0.90–1.00, respectively. However, vitrinite reflectance and its equivalent values (% Rc) should be used with caution in the SCB since possible overpressure build up caused by rapid sedimentation in the Middle Pliocene through Quaternary (Tagiyev et al., 1997) could be caused retardation (Dalla Torre, Mahlman, & Ernst, 1997; Zou and Peng, 2001).

In this study, we used 'depth-geothermal gradient-vitrinite reflectance' diagram of Suggate (1998), which helps to estimate the generation depth and corresponding temperatures intervals when geothermal gradient of the area and % Rc values of the oils are known. Representative geothermal gradient value for the region was calculated as 18 °C/1000 m from the recently drilled well nearby the oil sample locations when surface temperature of 18 °C assumed. These values (% Rc = 0.56–0.85; Geothermal gradient = 18 °C/1000 m) are plotted on the depth-geothermal gradient-vitrinite reflectance diagram as shown in Fig. 10. Following this, we estimate the source rock generation depth interval of approximately 5200 m (112 °C) to 7500 m (153 °C). Similar generation depth intervals were also observed when the % Rc values calculated in this study are plotted on the regional maturity profile diagram (Depth vs. % Ro) for the SCB established by

Wavrek et al. (1996). Depending on the different method of calculations and study areas, generation depth and temperature intervals of this study are slightly different than the previous estimations. Hydrocarbon generation depth intervals reported by Inan et al. (1998), Katz et al. (2000), and Wavrek et al. (1996) are 6400–8000 > 10,000 m, and > 5000 m, respectively. Notice the lack of consistencies among the values. Generation temperature intervals of the SCB oils range from 135 to 145 °C (Abdullaev et al., 1998), which is close to our values excluding generation depth of

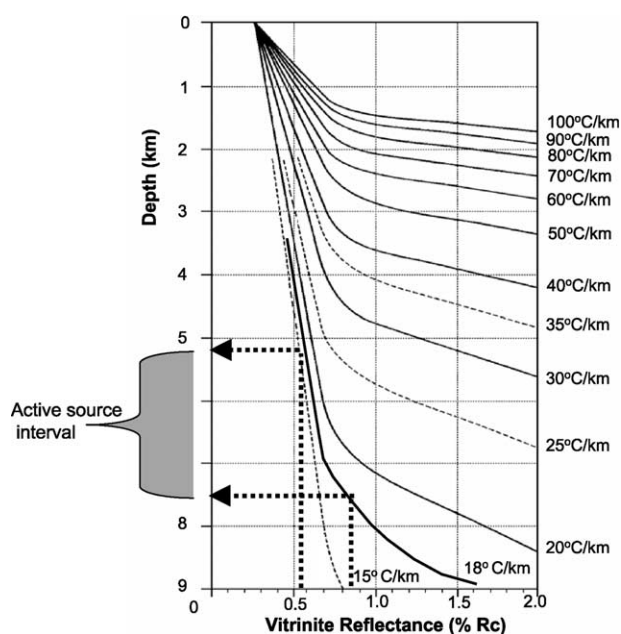


Fig. 10. Estimation of source kitchen depth for the GCA, Bahar, Gum adasi field oils on the basis of depth vs. vitrinite reflectance vs. geothermal gradient diagram of Suggate (1998).

5200 m for the GA-7 oil. These findings imply that any hydrocarbon generated from at a depth of 7500 m would have to migrate vertically at least 2200–4500 m through the Oligocene, Miocene and the lowest portion of the MPPS reservoirs.

4.2.3. Biodegradation

Biodegradation of oils occurs when temperature of reservoir is less than 80 °C, supply of oxygen is provided by meteoric water, and the aerobic bacteria are present. Many authors have observed that *n*-alkanes are utilized first by the bacteria then acyclic isoprenoid alkanes, and alkyl cycloalkanes while the lower molecular weight compounds are preferably consumed. Steranes and terpanes, which are the most commonly used biological marker alkanes for correlation and characterization purposes, are only consumed in very extreme cases (Connan, 1984; Seifert & Moldowan, 1979). Severely biodegraded oils show no-alkane peaks but displays various humps of sizes representing the ‘unresolved complex mixture’ (UCM), which consists of compounds resistant to biological attack. Thus, *n*-alkanes are commonly used for an early assessment of biodegradation effect on crude oils. For this purpose, representative gas chromatograms of each oil type are given in Fig. 11.

The Type 2A and 2B oils reflect very early stage of biodegradation on the basis of increase content of methylcyclohexane (MCH), toluene and xylene relative to their *n*-alkane counterparts (Figs. 11b and 12c). Within the Type 1, the Guneshli field oils clearly show degraded oil characteristics on the basis of presence of noticeable UCM and higher concentration of acyclic isoprenoids (e.g. Pr, Ph, *i*-C₁₆, *i*-C₁₈, and *i*-C₂₁) relative to their *n*-alkane homologous (Fig. 11a). As previously mentioned, high Pr/*n*-C₁₇ (10.62–33.33) and Ph/*n*-C₁₈ ratios (7.55–20.48) of the Guneshli oils reflect biodegradation (Fig. 6; Table 1). These characteristics correspond to moderate degrees of biodegradation using Peter and Moldowan’s (1993) scale (level 4). In this case, microbial alteration of gases from the Guneshli field reported by Katz, Narimanov, and Huseinzadeh (2002) appears to occur at the same time interval with the oils. Stepwise decrease of *n*-alkanes in Fig. 11a from *n*-C₁₂ to *n*-C₉ in the Guneshli oil is most likely caused by storage and/or laboratory loss. It is believed that sterane and terpane biomarkers in the Guneshli oils used for correlation purposes appear to be not affected by this level of biodegradation and probably keep their primary compositions. However, the presence of high concentration of light hydrocarbons (*n*-C₉ to *n*-C₁₆) in the Guneshli oils (Fig. 11a) is apparently contradictory to expected progress of biodegradation processes. This is evidence of an additional charge of light hydrocarbon input into biodegraded Guneshli oils.

An event chart showing hydrocarbon generation stages (Fig. 12; Yüklér, 1993, personal communication) has been used for delineation of the history of the biodegradation

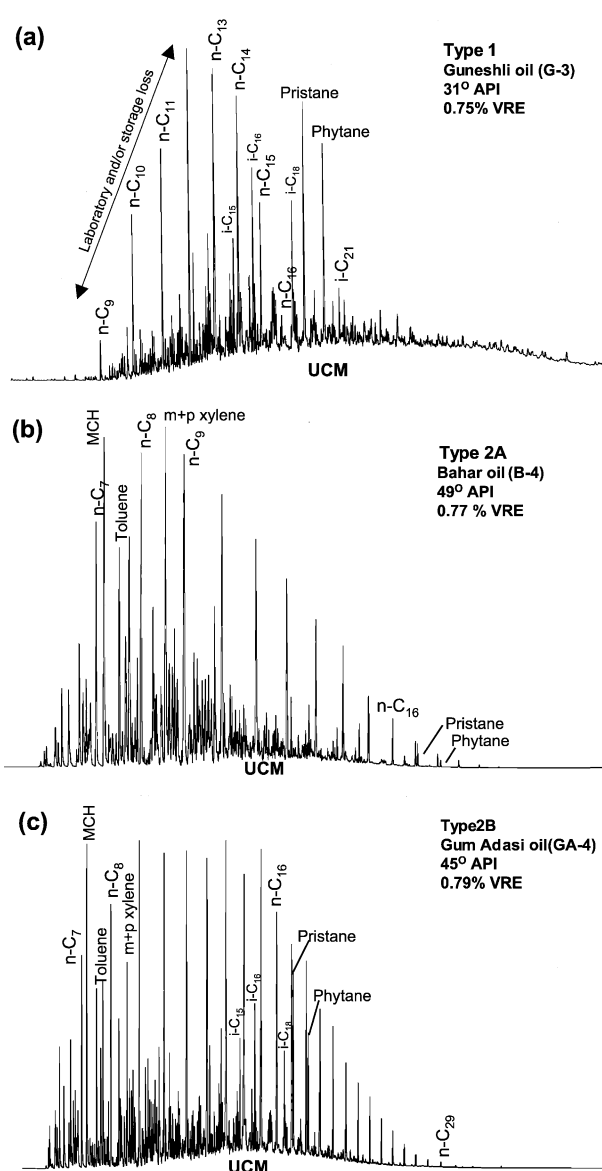


Fig. 11. Capillary gas chromatograms of selected oil samples from the South Caspian Basin: (a) Guneshli oil, (b) Bahar oil, and (c) Gum Adasi oil. Sample codes as in Tables 1 and 2.

process in the Guneshli field. The following sequential events might be occurred: generation and expulsion of relatively mature hydrocarbons (0.75–0.85% Rc; Table 2) from the relevant source rocks and subsequent migration and accumulation in the MPPS reservoirs approximately 2.3–1.9 mybp interval (main oil generation stage; Fig. 12). At the same time, intense Late Caucasus tectonic activity and the new mud diapirism caused significant uplift, trap formation, and subsequent erosions from the MPPS (Narimanov, 1993; Smale et al., 1997). During the 1.6 mybp hiatus between 4.2 and 2.6 mybp, oxygenated meteoric water carrying aerobic bacteria migrated along unconformities into Guneshli field oils. Bacteria first consume the *n*-alkanes of the light Guneshli oils, which

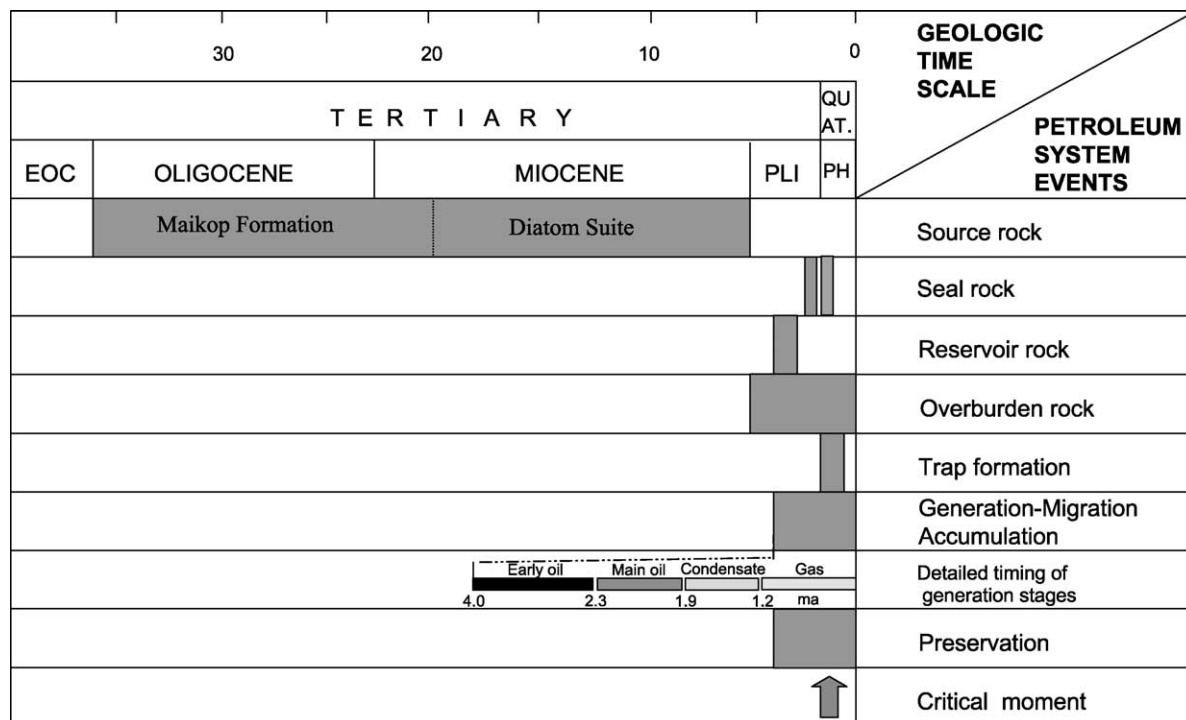


Fig. 12. Event chart showing significant time intervals for oil and gas generation stages in the study area.

left behind the relatively heavy oils. Presence of undegraded biomarker molecules in the analyzed Guneshli oils implies that biodegradation process took very short time and was not intense. Cessation of biodegradation occurred when the deposition of the thick and impermeable Akchagyl shale, which acts as a major seal in the study area, did not let meteoric water to flow down through the MPPS. Subsequently, light hydrocarbons were added to biodegraded and heavy Guneshli oils via deep-seated axial faults in 1.9–1.2 mybp. Narrow range of maturities among the Guneshli oils (Table 2; Figs. 8 and 9) indicates that primary biodegraded and subsequently added light hydrocarbons into the Guneshli field most likely share similar maturities.

An input of latter stage of light hydrocarbons into the earlier biodegraded heavy oils as seen in the Guneshli field is a widespread phenomena and has been well documented in several regions of the world: North Slope, Alaska (Masterson, Dzou, Holba, Fincannon, & Ellis, 2001) and Gulf of Mexico (Holba et al., 1996), Eastern Carpathians, Poland (Matyasik, Steczko, & Philp, 2000) and in the Umbaki field oils, western SCB (Abrams & Narimanov, 1997).

4.2.4. Origin of light hydrocarbons

Abrams and Narimanov (1997) suggested that the process called as 'evaporative-fractionation' is a valid way of explaining presence of light fractions in the biodegraded the SCB oils. However, origin of the light hydrocarbons in the Guneshli oils and Bahar field condensates can be one of these multiple sources: (1) cracking of kerogen in the source

rock, (2) cracking of oil in the reservoir, (3) early generation from resinite, (4) fractionation of normal oils upon a pressure release, i.e. evaporative-fractionation, and (5) organic matter subjected to high heating rates (>6.0 °C/my). Therefore, an attempt was made to investigate which of the above mechanism and/or mechanisms are responsible for the presence of the light hydrocarbons in the Guneshli field oils in the Bahar field condensates.

1. Cracking from kerogen can be easily ruled out, because in typical basins, kerogen cracking in the source rock requires vitrinite reflectance values around 1.20–1.80% Ro (Hunt, 1996) and temperature values around 155–205 °C depending on the hydrogen index and heating rates (Pepper & Dodd, 1995). As shown in previous discussions, generation temperatures of the Bahar field oils from the source rocks are found to be less than 155–205 °C.
2. Reservoir cracking is also negligible since this process occurs at temperatures around 174–195 °C depending on the composition of oil as exemplified in North Sea (Pepper & Dodd, 1995). The depth intervals of the PS in the Bahar field vary between 2800 and 5500 m (Narimanov et al., 1998) that correspond temperatures between 80 and 120 °C (Abrams & Narimanov, 1997). This also indicates that formation of Bahar condensates has not been occurred as a result of oil cracking in the reservoirs.
3. Early generation from resinite-rich organic matter (Snowdon & Powell, 1982) can be also ruled out

since the major source of the region's oils, Oligocene–Early Miocene Maikop and Diatom Suite samples, do not contain resinite rich organic matter but regular Type II marine organic matter (Abrams & Narimanov, 1997).

Evaporative-fractionation has been observed in many locations around the world, at the US Gulf Coast (Meulbroek, Cathles III, & Whelan, 1998; Thompson, 1987), the South China Sea (Quansing & Quaming, 1991), the North Sea (Larter & Mills, 1991), offshore Taiwan (Dzou & Hughes, 1993), Columbus Basin, Trinidad (Ross & Ames, 1988), and offshore Alaska (Kvenvolden & Claypool, 1980; Masterson et al., 2001). This process initiates with the intersection of an active fault (newly formed or re-activated fault) with a gas/condensate saturated oil (pristine oil) reservoir. When this occurs it is postulated that only the saturated light hydrocarbons migrates vertically (migrant oil) along the fault planes. Relatively heavy oil that is resulted from removal of the light migrant oil from the original pristine oil is called as 'residual oil'. As understood, evaporative-fractionation has mainly three components, migrant oil, residual oil, and pristine oil. It is also noted that evaporative-fractionation is a dynamic process therefore composition of its components changes as the intensity of the process increases. For example: the residual oils show deficiency of light *n*-alkanes, (the phenomenon introduces uncertainty as to whether the light-end loss is natural or an artifact of production or storage) yet possessing abnormally high concentrations of light aromatic hydrocarbons, particularly benzene, toluene, *meta*-xylene, and *para*-xylene, and of light cycloalkanes, particularly methylcyclopentane, cyclohexane, and methylcyclohexane and they are heavier compare to pristine oils. The migrant oil, on the other hand, represents high concentration of light-end *n*-alkanes, low concentration of light aromatics, and cycloalkanes and they are light oils compare to residual and pristine oils.

In the light of summary given above, the light hydrocarbon fraction (from *n*-C₉ to *n*-C₁₆) in the Guneshli oils appears to be a migrant component of a primary oil accumulated in the deeper portion of the Guneshli field. However, further evidence is necessary from the *n*-C₉ (–) light hydrocarbons to relate the presence of light hydrocarbon fraction (*n*-C₉ to *n*-C₁₆) in the Guneshli oils to evaporative-fractionation mechanism. Somewhat surprising, however, is that the Guneshli oils plotting out of 'typical crude oil area' in Fig. 4 also show very high resin to asphaltene ratios (e.g. low asphaltene contents) the main cause of which is believed to be precipitation of asphaltenes upon the second charge of light hydrocarbons into the MPPS reservoirs. Asphaltene residues observed in certain levels of the MPPS reservoirs in the Guneshli field (Riley, 2003 personal communication) support the occurrence of asphaltene precipitation in this particular oil field. A likely

mechanism for condensate leakage may be provided by deep-seated axial faults that remove hydrocarbons from the deep reservoirs. The faults that had connected the deeply accumulated oil reservoirs and the Guneshli reservoirs appear to be closed to oil and gas migration at present. If oil and gas migration were leaking up the faults today, *n*-alkanes heavier than the gas–condensates range would be present in the Guneshli oils. Unfortunately, *n*-C₉ (–) light hydrocarbons in the Guneshli oils are missing due to lost during storage and/or laboratory work (Fig. 11a). However, a further attempt was made on the characteristics of the Type 2A and 2B oils to examine any sign of evaporative-fractionation.

Thompson (1987) used 'aromaticity' B parameter (toluene/*n*-C₇) vs. 'parafinicity' F parameter (*n*-C₇/MCH) diagram to assess components of evaporative migration process. He showed that B parameter increases with increasing loss of light hydrocarbons from relevant pristine oil whereas F parameter increases with increasing maturity. These relations for the Type 2A and 2B oils are shown in Fig. 13a where the Type 2A and 2B oils follow different trends. For the Type 2B oils, F parameter increases with increasing B parameter suggesting that the Type 2B oils are neither pristine nor residual oil components. This finding is further supported by the smooth *n*-C₉ to *n*-C₃₁ distribution on the gas chromatograms of the Type 2B oils (Fig. 5c). However, the trend observed for the Type 2B oils in Fig. 13a is exactly similar to the trend between B parameter and % Rc values (Fig. 13b). When the organic matter type effect on the B parameter is tested on a B parameter vs. C₂₇/C₂₉ sterane ratio diagram (Fig. 13c) very small changes in the C₂₇/C₂₉ sterane ratio relative to B parameter was found. This suggests that the type of organic matter does not affect B parameter.

In contrast to the Type 2B oils, F parameter decreases with increasing B parameter for the Type 2A oils, which may be used as an indicator for the evaporative-migration as samples B-3 and B-5 are the residual oils and samples B-4 and B-2 are pristine oils (Fig. 13a). If this observation were correct than the residual oils, B-3 and B-5 should have been heavier than the pristine B-2 and B-4 oils. However, it is not the case since the four oils have similar API gravities (Table 2). In addition, on the B parameter vs. % Rc diagram (Fig. 13b, the trend direction from the oil samples B-4 and B-2 to B-5 and B-3 is similar to trend in Fig. 13a that points out that this trend is also influenced by maturity (Fig. 13b). Similar feature is also observed in Fig. 13c, which indicates that, the trend in Fig. 13a for the Type 2A oils parallel to that between B parameter vs. C₂₇/C₂₉ sterane ratio. This is also a good indication of organic matter effect on the Thompson (1987) diagram. Similarly, Leythaeuser, Schaefer, Conford, & Weiner (1979) reported that higher plants contain relatively higher proportion of benzene and toluene than the organic matter of marine origin.

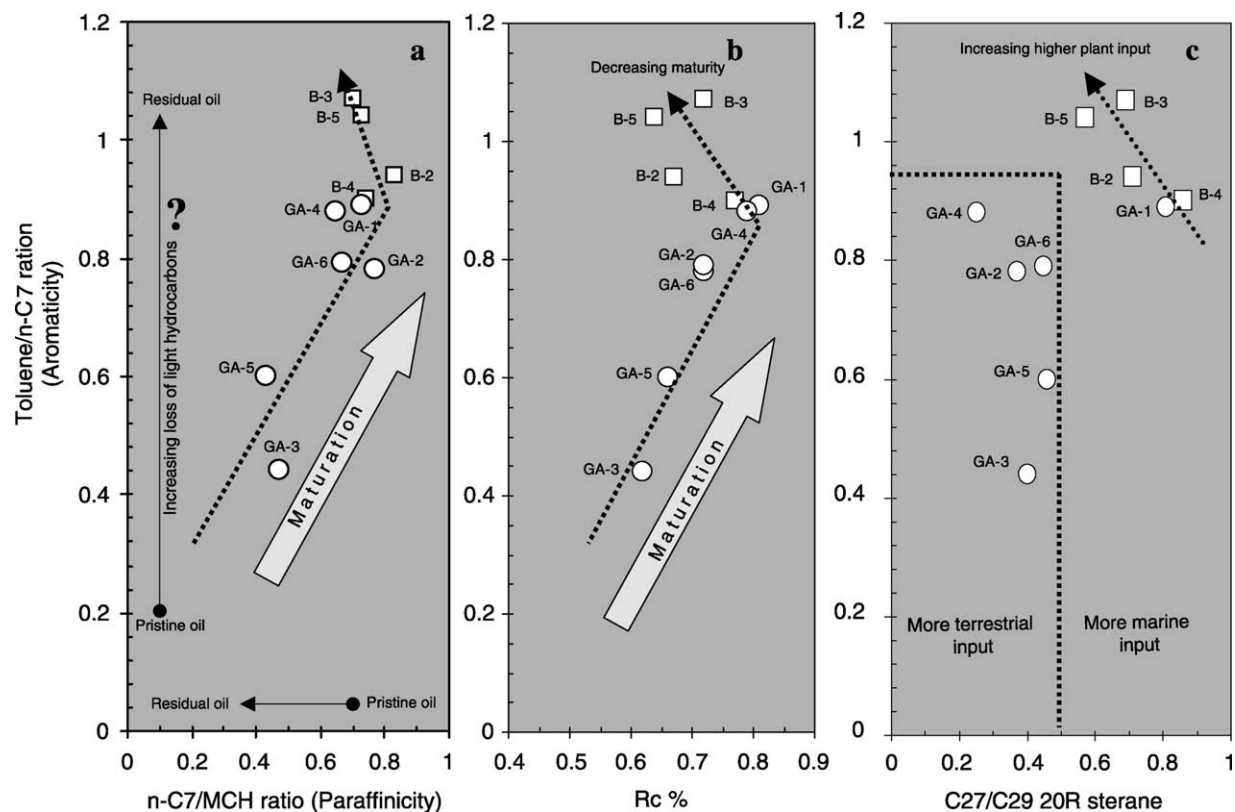


Fig. 13. An attempt to assess 'evaporative fractionation' process on the Bahar and Gum Adasi field oils: (a) B parameter, Aromaticity (toluene/ n -C₇) vs. F parameter, Paraffinity (n -C₇/MCH) (after Thompson, 1987), (b) B parameter, Aromaticity (toluene/ n -C₇) vs. %Rc, and (c) B parameter, Aromaticity (toluene/ n -C₇) vs. C₂₇/C₂₉ 20R sterane ratio. Sample codes as in Tables 1 and 2.

Therefore, it is proposed here that Thompson (1987) diagram constructed based on B vs. F parameters should be used in caution since both parameters are affected by maturity as well as organic matter type in addition to evaporative-fractionation process. However, without analyzing and having sufficient data on the pristine oils of the analyzed oils, it would be difficult to evaluate whether or not the Guneshli, Bahar and Gum Adasi oils undergone evaporative-fractionation process.

- High heating rate (>6 °C/my) is also a significant mechanism to generate condensates at very early stage of thermal maturation if source rock contains sufficient oil prone organic matter with high TOC content. The timing of the main hydrocarbon stages of the study area calculated using the Yüklér quantitative basin analysis program (Fig. 12; Yüklér, 1993 personal communication) coincides with periods of high sedimentation rate (to 1300 m/my; Tagiyev et al., 1997) of Pliocene sediments and high heating rate (to 24–40 °C/my; Yüklér, 1993 personal communication). Presence of the early formation of light hydrocarbons and condensates in the SCB is not surprising since a study of hydrocarbon generation vs. % Ro as a function of heating rate diagram for 12 basins around the world has shown that high heating rate plays a significant role in the early generation and expulsion of large range of hydrocarbons

(e.g. oil + condensate + gas) (Yüklér, 1992 personal communication). For example, high heating rates were recorded at the Hod-1 well (Pannonian Basin, Hungary), where main-stage oil generation occurs at present at 0.64% Ro. Gürgey (1999) also showed that onset of oil generation began at 0.52% Ro and 0.45% Ro in the Thrace basin (NW Turkey) and western Turkmenistan, respectively. Further supporting evidence by Sajgo et al. (1988) indicates that the main oil generation zone determined from a depth vs. extract (%) diagram corresponds to region $<0.70\%$ Ro. In short, it is believed that formation of the light hydrocarbons in the Guneshli field and condensates in the Bahar field were significantly influenced by the rapid burial of the Pliocene sediments and subsequent high heating rate on the organic matter in possible deeper source rocks.

5. Implications for source rock distributions

In the SCB, Pliocene and Pleistocene units show insufficient maturity to generate significant volume of hydrocarbons (Fig. 10). Hence, these units have not been considered as source rock candidates for the western SCB oils.

Devlin et al. (1999) reported that organic rich units in the SCB are calcareous and diatomaceous black shales of

the Oligocene–Lower Miocene Maikop Formation and the Middle–Upper Miocene Diatom Suite. These units were deposited in euxinic and restricted marine conditions created by the collision of the Arabian and Eurasian plates in the Late Paleogene. Palynological, paleontological, and sedimentological evidence indicate that the Maikop Formation is a regressive unit characterized by upwardly-increasing terrestrial input (Jones & Simmons, 1996). If so, the Diatom Suite stratigraphically being part of the upper portion of the Maikop system should contain substantial amount of terrestrial organic matter. This approach is supported by Katz et al. (2000) who reported that onshore Diatom Suite samples are organically poor and contain abundant Type III organic matter. Guliev and Feizullayev (1996) analyzed, outcrop, mud volcano ejecta, and core samples from onshore Azerbaijan and found that the Lower Miocene Maikop Formation ($n = 1446$ and $\text{TOC}_{\text{mean}} = 0.69$ wt.%) and the Middle–Upper Miocene Diatom Suite ($n = 639$ and $\text{TOC}_{\text{mean}} = 0.59$ wt.%) has low source rock potential. Bailey et al. (1996) reported that extracts of the Maikop Formation and Diatom Suite from onshore Azerbaijan show low Pr/Ph ratios of less than 0.60. As far as regional oil-to-source rock correlations are concerned, Pr/Ph ratios of the onshore extracts and those of the offshore Azerbaijan oils (western SCB oils; Table 1) from this study are not correlative.

The Maikop Formation and Diatom Suite appear to be less likely source of the offshore Azerbaijan oils based on their organic facies and organic richness of the onshore outcrop samples. It is believed that being an effective source rocks for offshore Azerbaijan oils require significant changes in organic facies towards to the offshore areas. Devlin (2000) brought similar hypothesis and pointed out that source quality and organic richness of the Maikop Formation and Diatom Suite should increase from more proximal onshore localities in the west to more distal, basinal settings in the area of the present-day SCB. The Maikop Formation has been divided into three sub-units: Lower Maikop, Middle Maikop, and Upper Maikop (fig. 8 of Abrams & Narimanov, 1997). Abraham and Narimanov (1996) also noted that oils produced from MPPS and younger reservoirs were most likely derived from Middle, Upper Maikop and Diatom suite whereas oils produced from reservoirs older than Pliocene were probably derived from the Lower Maikop Formation. This narrowed the possible source rocks for MPPS oils in the offshore areas to the Middle and Upper Maikop Formation and Diatom Suite. However, source quality and organic richness of these source candidates have not been proved yet since both units have not been penetrated in the offshore area of Azerbaijan. Despite the lack of data on the source rock candidates, we tend to assume that the Maikop Formation and Diatom Suite are the effective source rocks in the western SCB.

Preceding discussion on oil-to-oil correlations shows that there are two major oil types in the western SCB implying presence of at least two different major source rocks. We

believe that base on the geochemical attributes of the Type 1 oils (GCA) analyzed in this study, source rock of the GCA field oils is probably the basinal shales of the Middle Maikop Formation with less terrestrial input.

Type 2 oils (Bahar and Gum Adasi fields) seem to be generated from the shales of the Upper Maikop Formation and Diatom Suite. Type 2A oils (Bahar field oils) with high terrestrial input might be derived from the shelf-edge setting of the Upper Maikop and Type 2B oils (Gum Adasi field oils), on the other hand, might be sourced from the diatomaceous shales of the shelf-edge setting of the Diatom Suite.

6. Summary and conclusions

Organic geochemical data generated from Iatro-scan, GC, and GC-MS analyses of 20 crude oil samples from Middle Pliocene Production Series (MPPS) of Guneshli-Chirag-Azeri (GCA), Bahar, and Gum Adasi fields, western South Caspian Basin (SCB), were assessed. The following conclusions were accomplished:

1. Source of the analyzed oils is most likely Tertiary marine shales containing a mixed higher plant and marine algal organic matter deposited under an oxic- to sub-oxic bottom water conditions.
2. Application of multivariate statistical analysis (PCA) to the source-specific biomarker dataset revealed two distinct oil types with one being divided into two sub-types: the eight oils from GCA fields (Type 1), five oils from Bahar (Type 2A), and seven oils from the Gum Adasi (Type 2B) fields. Type 1 oils, located in the Apsheron-Balkhans uplift area, are derived probably from basinal shales of the Oligocene–Lower Miocene Upper Maikop Formation and diatomaceous shales of the Middle–Upper Miocene Diatom Suite. Type 2A and 2B oils, located in the Gum-deniz-Bahar-Shakh-deniz trend area, are more likely derived from shelf-edge and slope shales of the Middle Maikop Formation.
3. The Type 1 oils (mean % Rc = 0.78) appear to be more mature than the Type 2 oils (mean % Rc = 0.71). Extrapolation of the calculated thermal maturity values (0.56–0.85% Rc) on the Suggate (1998) diagram suggests a source depth interval from 5200 m (112 °C) to 7500 m (153 °C) at the time of expulsion. This implies that GCA, Bahar and Gum Adasi field oils analyzed in this study subjected to significant distance (2000–3000 m) of vertical migration.
4. Following low level of biodegradation (level 4) of the primary Guneshli oils, light hydrocarbons (C_1 – C_{16}) were added into the reservoirs. As a result, deasphaltenig occurred and asphaltene content of the Guneshli fields decreased.
5. Approach of Thompson (1987) should be used with caution for the SCB oils since both F and B parameters

are affected by organic matter type and maturity accumulations in the SCB.

6. Rapid burial and subsequent heating rate more likely caused the formation of light hydrocarbons present in the Guneshli oils and condensates in the Bahar field.
7. Successful application of multivariate statistical approach to correlate closely similar SCB oils has been performed. These allow us, for the first time, an assignment of each individual oil field to a specific source unit.

Acknowledgements

Permission to publish these results by Orhan Duran (TPAO Foreign Exploration Group, Ankara) is gratefully acknowledged. Ayse Yildirim and Sema Sayılı and Yesim Bizim from the TPAO Research Center-Geochemistry Department are thanked for their analytical support during the research. Special thanks to Drs Cengiz Soyulu and Zühtü Bati for reviewing an early draft. I would particularly like to thank an anonymous referee and D.G. Roberts for their very constructive comments.

References

- Abdullaev, T., Falt, M. L., Akhundov, A., van Grass, W. G., Kwamme, T., Flolo, H. L., Mehmedarov, K., Narimanov, A. A., Olsen, S. T., Seljeskog, G., Skontorp, O., Sultanzade, T., Tank, N., & Valieva, E. (1998). A reservoir model for the main Pliocene reservoirs of the Bahar Field in the Caspian Sea. Azerbaijan. *Petroleum Geoscience*, 4, 259–270.
- Abrams, A. M., & Narimanov, A. A. (1997). Geochemical evaluation of hydrocarbons and their potential sources in the western South Caspian depression, Republic of Azerbaijan. *Marine and Petroleum Geology*, 14, 451–468.
- Bagirov, E., Nadirov, R., & Lerche, I. (1998). Hydrocarbon evaluation for a north–south section of the South Caspian Basin. *Marine and Petroleum Geology*, 14, 773–854.
- Bailey, N. J. L., Guliyev, I., & Feizullayev, A. A. (1996). *Source rocks in the South Caspian*. In AAPG/ASPG Research Symposium on oil and gas petroleum systems in rapidly-subsiding basins, Baku, Azerbaijan, October 6–9.
- Bredehoeft, D. J., Djevanshir, R. D., & Belitz, K. R. (1988). Lateral fluid flow in a compacting sand-shale sequence: South Caspian Basin. *American Association of Petroleum Geologists Bulletin*, 72, 416–424.
- Connan, J. (1984). Biodegradation of crude oils in reservoirs. In J. Brooks, & D. H. Welte (Eds.), (Vol. 1) (pp. 299–335). *Advances in petroleum geochemistry*, London: Academic Press.
- Connan, J., & Cassau, A. M. (1980). Properties of gas petroleum liquids derived from terrestrial kerogen at various maturation levels. *Geochimica Cosmochimica Acta*, 44, 1–23.
- Dahl, J., Moldowan, M. J., Teerman, C. S., McCaffrey, A. M., & Sundararaman, P. (1994). Source rock quality determination from oil biomarkers I: a new geochemical technique. *American Association of Petroleum Geologists Bulletin*, 78, 1507–1526.
- Dalla Torre, M., Mahlman, R. F., & Ernst, W. G. (1997). Experimental study on the pressure dependence of vitrinite maturation. *Geochimica Cosmochimica Acta*, 61, 2921–2928.
- Davis, C. J. (1973). *Statistics and data analysis in geology*. New York: Wiley, p. 550.
- Devlin, J. W. (2000). *Hydrocarbon system of reservoir oils in the South Caspian*. In American Association of Petroleum Geologists, Inaugural Regional International Conference, Istanbul, Turkey, July 9–12.
- Devlin, J. W., Cogswell, J. M., Gaskins, G. M., Isaksen, G. H., Pitcher, D. M., Puls, D. P., Stanley, K. O., & Wall, G. R. T. (1999). South Caspian basin: young, cool and of promise. *GSA Today*, 9, 1–9.
- Didyk, B. M., Simoneit, B. R. T., Brasell, S. C., & Englinton, G. (1978). Organic geochemical indicators of paleoenvironmental conditions of sedimentation. *Nature*, 272, 216–222.
- Djevanshir, R. D., & Mansoori, A. G. (2000). Editorial: introduction to South Caspian Basin special issue. *Journal of Petroleum Science and Engineering*, 28, 153–155.
- Djavadova, S. A., Narimanov, A. A., & Rinaldi, G. G. (1997). *Biomarker hydrocarbon studies and geological interpretations, South Caspian depression, Azerbaijan*. In EAGE 59th Conference and Technical Exhibition—Geneva, Switzerland 26–30.
- Dzou, P. I. L., & Hughes, W. B. (1993). Geochemistry of oils and condensates, K Field, offshore Taiwan: a case study in migration fractionation. *Organic Geochemistry*, 20, 437–462.
- Eneogwe, C. (2003). Geochemical correlation of crude oils in the NW Niger Delta, Nigeria. *Journal of Petroleum Geology*, 26, 95–103.
- Grantham, P. J., & Wakefield, L. L. (1988). Variations in the sterane carbon number distributions of marine source rock derived crude oils through geologic time. *Organic Geochemistry*, 12, 61–73.
- Grantham, P. J., Posthuma, J., & Baak, A. (1983). Triterpanes in a number of far-eastern crude oils. In Bjroy, et al. (Eds.), (pp. 675–683). *Advances in Organic Geochemistry 1981*, New York: Wiley.
- Grantham, P. J. (1986). Sterane isomerization and moretane/hopanes ratios in crude oils derived from tertiary source rocks. *Organic Geochemistry*, 12, 495–506.
- Guliev, I. S., & Feizullayev, A. A. (1996). Geochemistry of hydrocarbon seepages in Azerbaijan. In Schumacher, & Abrams (Eds.), *Near Surface Expression of Hydrocarbon Migration (66)* (pp. 63–70). AAPG memoir.
- Gürgey, K. (1999). Geochemical characteristics and thermal maturity of oils from the Thrace Basin (northwestern Turkey) and western Turkmenistan. *Journal of Petroleum Geology*, 22, 167–189.
- Holba, A. G., Dzou, P. I. L., Hickey, J. J., Franks, G. G., May, S. J., & Lenney, T. (1996). Reservoir geochemistry of South Pass 61 Field Gulf of Mexico: compositional heterogeneties reflecting filling history and biodegradation. *Organic Geochemistry*, 24, 1179–1198.
- Huang, W. Y., & Meinschein, W. G. (1979). Sterols as ecological indicators. *Geochimica Cosmochimica Acta*, 43, 739–745.
- Hunt, M. J. (1996). *Petroleum geochemistry and geology*. New York: Freeman, p. 393.
- Inan, S., Yalcin, N. M., Guliev, S. I., Kuliev, K., & Feizullayev, A. A. (1998). Deep petroleum occurrences in the Lower Kura depression, South Caspian Basin, Azerbaijan. An organic geochemical and basin modelling study. *Marine and Petroleum Geology*, 14, 731–762.
- Johnson, L. C., Greene, J. D., Zinniker, A. D., Moldowan, M. C., Hendrix, S. M., & Carroll, R. A. (2003). Geochemical characteristics and correlation of oil and nonmarine source rocks from Mongolia. *American Association of Petroleum Geologists Bulletin*, 87, 817–846.
- Jones, W. R., & Simmons, D. M. (1996). A review of the stratigraphy of Eastern Paratethys (oligocene–holocene). *Bulletin of Natural History Museum, London (Geology)*, 52, 25–49.
- Katz, K. J., Narimanov, A., & Huseinzadeh, R. (2002). Significance of microbial processes in gases of the South Caspian basin. *Marine and Petroleum Geology*, 19, 783–796.
- Katz, K. J., Richards, D., Long, D., & Lawrence, W. (2000). A new look at the components of the petroleum system of the South Caspian Basin. *Journal of Petroleum Science and Engineering*, 28, 161–182.
- Kvenvolden, K. E., & Claypool, G. E. (1980). Origin of gasoline-range hydrocarbons and their migration by solution in carbon dioxide in

- Norton Basin, AK. *American Association of Petroleum Geologists Bulletin*, 64, 1078–1106.
- Leythaeuser, D., Schaefer, R. G., Conford, C., & Weiner, B. (1979). Generation and migration of light hydrocarbons (C₂–C₇) in sedimentary basins. *Organic Geochemistry*, 1, 191–204.
- Larter, S., & Mills, N. (1991). Phase controlled molecular fractionations in migrating petroleum charges. In England, & Fleet (Eds.), *Petroleum migration, Geological Society Special Publication*, 59, London (pp. 137–147).
- Mackenzie, A. S. (1984). Applications of biomarkers in petroleum geochemistry. In J. Brooks, & D. H. Welte (Eds.), (Vol. 1) (pp. 115–214). *Advances in petroleum geochemistry*, London: Academic Press.
- Mackenzie, A. S., Patience, R. L., & Maxwell, J. R. (1980). Molecular parameters of maturation in the Toarcian shales, Paris Basin France-I. Changes in the configurations of acyclic isoprenoid alkanes, steranes and triterpanes. *Geochimica Cosmochimica Acta*, 44, 1709–1721.
- Masterson, W. D., Dzou, L. P. I., Holba, A. G., Fincannon, A. L., & Ellis, L. (2001). Evidence for biodegradation and evaporative-fractionation in West Sak, Kuparuk and Prudhoe Bay field areas, North slope, Alaska. *Organic Geochemistry*, 32, 411–441.
- Matyasik, I., Steczko, A., & Philp, R. P. (2000). Biodegradation and migrational fractionation of oils and condensates from the Eastern Carpathians, Poland. *Organic Geochemistry*, 31, 1509–1523.
- Meulbroek, P., Cathles, L. A., III, & Whelan, J. (1998). Phase fractionation at south Eugene Island Block 330. *Organic Geochemistry*, 29, 223–239.
- Narimanov, A. A. (1993). The petroleum system of the South Caspian Basin. In Dore, et al. (Eds.), *Basin modelling: advances and applications (Vol. 3)* (pp. 599–608). *NPF Special Publication*, Amsterdam: Elsevier.
- Narimanov, A. A., Akperov, A. N., & Abdullaev, I. T. (1998). The Bahar oil and gas–condensate field in the South Caspian. *Petroleum Geoscience*, 4, 253–258.
- Palacas, G. P., Anders, D. E., & King, J. D. (1984). South Florida Basin-A prime—example of carbonate source rocks of petroleum. In Palacas (Ed.), *In Petroleum Geochemistry and Source Rock Potential of Carbonate Rocks* (pp. 71–96). *AAPG studies in geology* 18.
- Pepper, A. S., & Dodd, T. A. (1995). Simple kinetic models of petroleum formation. Part II: oil–gas cracking. *Marine and Petroleum Geology*, 12, 321–340.
- Peters, K. E., & Moldowan, J. M. (1993). The Biomarker Guide: interpreting molecular fossils in petroleum and ancient sediments. Englewood Cliffs, NJ: Prentice-Hall, p. 254.
- Peters, E. K., Frase, H. T., Amris, W., Rustanto, B., & Hermento, E. (1999). Geochemistry of crude oils from Eastern Indonesia. *American Association of Petroleum Geologists Bulletin*, 83, 1927–1942.
- Philp, R. P., & Gilbert, T. D. (1986). Biomarker distribution in oils predominantly derived from terrigenous material. In Leythaeuser, & Rullkötter (Eds.), (1985) (pp. 73–84). *Advances in Organic Geochemistry*, Pergamon: Pergamon Press.
- Powell, T. G., & Mckirdy, D. M. (1973). Relationship between ratio of pristane to phytane, crude oil composition, and geological environment in Australia. *Nature*, 243, 37–39.
- Quansing, Z., & Quaming, Z. (1991). Evidence of primary migration of condensate by molecular solution in aqueous phase in Yacheng field, offshore South China. *Journal of Southeast Asian Earth Sciences*, 5, 101–106.
- Ramon, J. C., & Dzou, I. L. (1999). Petroleum geochemistry of Middle Magdalena Valley, Colombia. *Organic Geochemistry*, 30, 249–266.
- Ross, M. L., & Ames, L. R. (1988). Stratification of oils in Columbus basin off Trinidad. *Oil and Gas Journal*, September, 72–75.
- Rullkötter, J., Spiro, B., & Nissenbaum, A. (1985). Biological marker characteristics of oils and asphalts from carbonate source rocks in rapidly subsiding graben, Dead Sea, Israel. *Geochimica Cosmochimica Acta*, 49, 1357–1370.
- Sajgo, et al. (1988). An organic maturation study of the Hod-1 borehole (Pannonian basin). In Royden, & Horvath (Eds.), (Vol. 45) (pp. 297–309). *AAPG memoir*.
- Seifert, W. K., & Moldowan, J. M. (1978). Application of steranes, terpanes, monoaromatics to the maturation, migration, source of crude oils. *Geochimica Cosmochimica Acta*, 42, 77–95.
- Seifert, W. K., & Moldowan, J. M. (1979). The effect of biodegradation on steranes and terpanes in crude oils. *Geochimica Cosmochimica Acta*, 43, 111–126.
- Smale, J. L., Shikhaliyev, Y., & Beylin, T. I. (1997). Faulting and associated mud diapirism in the South Caspian Basin—implications for hydrocarbon trap development. *EAGE 59th Conference and Technical Exhibition Geneva, Switzerland, 26–30 May—petroleum division extended abstracts 2*, 1997.
- Snowdon, L. R., & Powell, T. G. (1982). Immature oil–condensate-modification of hydrocarbon generation model for terrestrial organic matter. *American Association of Petroleum Geologists Bulletin*, 66, 775–788.
- Suggate, P. R. (1998). Relations between depth of burial, vitrinite reflectance and geothermal gradient. *Journal of Petroleum Geology*, 21, 5–32.
- Tagiyev, F. M., Nadirov, S. R., Bagirov, B. E., & Lerche, I. (1997). Geohistory, thermal history, and hydrocarbon generation history of the north-west South Caspian basin. *Marine and Petroleum Geology*, 14, 363–382.
- Telnaes, N., & Dahl, B. (1985). Oil to oil correlation using multivariate techniques. *Organic Geochemistry*, 10, 425–432.
- Thompson, K. F. M. (1987). Fractionated aromatic petroleums and the generation of gas–condensates. *Organic Geochemistry*, 11, 573–590.
- Tissot, B. P., & Welte, D. H. (1984). Petroleum formation and occurrence (2nd ed). New York: Springer, p. 699.
- Van Grass, G. W. (1990). Biomarker maturity parameters for high maturities: calibration of the working range up to the oil/condensate threshold. *Organic Geochemistry*, 16, 1025–1032.
- Volkman, J. K., Alexander, R., Kagi, R. I., Noble, R. A., & Woodhouse, G. W. (1983). A geochemical reconstruction of oil generation in the Barrow sub-basin of western Australia. *Geochimica Cosmochimica Acta*, 47, 2091–2106.
- Waples, D. W., & Machihara, T. (1990). Application of sterane and triterpane biomarkers in petroleum exploration. *Bulletin of Canadian Petroleum Geology*, 30, 357–380.
- Wavrek, D. A., Collister, J. W., Curtiss, K. D., Quick, C. J., Guliyev, I. S., & Feyzullayev, A. A. (1996). Novel application of geochemical inversion to derive generation/expulsion kinetic parameters for the South Caspian petroleum system. In *AAPG/ASPG Research Symposium on oil and gas petroleum systems in rapidly-subsiding basins, Baku, Azerbaijan, October 6–9*.
- Zou, Y. R., & Peng, P. (2001). Overpressure retardation of organic-matter maturation: a kinetic model and its application. *Marine and Petroleum Geology*, 18, 707–713.
- Zumberge, J. E. (1987). Prediction of source rock characteristics based on terpane biomarkers in crude oils: Multivariate statistical approach. *Geochimica Cosmochimica Acta*, 51, 1625–1637.